arXiv:2605.15189v3 [astro-ph.CO] 1 Sep 2026

Strong Gravitational Lensing with the James Webb Space Telescope

Adi Zitrin[a]

[a]Department of Physics, Ben-Gurion University of the Negev, P.O. Box 653, Be'er-Sheva 8410501, Israel

ARTICLE HISTORY
Compiled September 2, 2026

ABSTRACT
The theory of General Relativity predicts that, since massive bodies curve spacetime, light from a distant source would be deflected by a foreground massive object – a phenomenon known as *Gravitational Lensing*. Historically, the strength of deflection of light from background stars by the sun, during the 1919 solar eclipse, supplied one of the first proofs for the theory of General Relativity. However, it is only in the last few decades, with the advent of the Hubble Space Telescope and other large, ground-based facilities, that lensing has become a principal tool in modern astronomy. Lensing allows us to study both the matter content of the lensing bodies such as galaxies or clusters of galaxies, mainly dominated by the otherwise-invisible *dark matter*, and the distant background sources that are being lensed by them. Strong gravitational lensing, where sources are substantially magnified and multiply imaged, is particularly useful to that end. The substantial magnification enables a high-resolution view of the sources and the detection of fainter and farther objects than would otherwise be possible; and image multiplicity helps in verifying the distance to them, and in studying variable or transient sources. Paired with the unprecedented capabilities of the James Webb Space Telescope (JWST), lensing now allows us to observe, detect, and study distant sources like never before. I summarise recent advances in strong-lensing applications and near-future prospects with JWST.

KEYWORDS
Strong gravitational lensing; galaxy clusters; dark matter; high-redshift galaxies; supernovae; star clusters; quasars; supermassive black holes; distant stars

1. Introduction

From everyday life to the distant Universe Sunsets, rainbows, stars, or the phases of the moon – the curious human has long been fascinated with optical phenomena. This is perhaps only natural, given that we perceive the world primarily through vision, and that these phenomena hold clues about our physical world. Indeed, optics is also a prominent field in physics, and light and its nature are fundamental to our physical Universe.

A magnifying glass in the hands of a child opens a world of marvellous possibilities. Through the lens, objects appear magnified, and in the case of more complex lenses, often seem distorted and appearing multiple times. It can be used to concentrate sunlight onto a spot - causing small burns on wood or in dry leaves, to observe tiny

CONTACT Adi Zitrin. Email: zitrin@bgu.ac.il

creatures, or to read miniscule letters written on a single grain of rice.

This review concentrates on a phenomenon which is often referred to as the astronomical parallel to the magnifying glass – *strong gravitational lensing*. I start with a brief history of gravitational lensing, followed by some qualitative description of the phenomenon and its different regimes. I then overview how, technically, (strong-) lensing is modelled and the range of science it facilitates; from studies of distant galaxies and black holes, through the nature of dark matter, to cosmology. I review how strong-lensing science has been established with the Hubble Space Telescope (HST, or *Hubble*) over the past 2-3 decades, and the shifts taking place since the launch of the James Webb Space Telescope (JWST), in particular towards studying small, point-like (stars, star clusters), varying (quasars) or exploding transient (supernovae (SNe)) sources. Since they are the most massive gravitationally bound objects in the Universe, this review concentrates in particular on strong lensing by *clusters of galaxies*, where most prominent lensing manifestations appear, although much of the science is also relevant for smaller lenses such as galaxies. I mention some recent advances from various cluster-lensing programs with JWST, together with some prospects for strong-lensing science in the near future with JWST, and for its interplay with recent or upcoming observatories from ground and space.

1.1. A brief history of gravitational lensing

If light were assumed to consist of some test particles (corpuscles), then – similar to other massive bodies – when passing near a massive astronomical body the particles should be attracted to it, and thus deflected with respect to their original trajectory. The acceleration the particles would experience is independent of their mass, and the strength of deflection, the *deflection angle*, can be calculated in the framework of Newtonian mechanics. This calculation is first attributed to Henry Cavendish in 1784, apparently following a letter by John Michell to him concerning the effect of gravity on the speed of light [1,2]. The Newtonian deflection angle comes out to be $\hat{\alpha} = \frac{2GM}{c^2 r}$, where G is the universal gravitational constant, c the speed of light, M the deflector's mass and r the distance of closest approach to it. For example, the deflection angle from the sun for a light ray passing right next to its surface, becomes $\approx 0".875$. Distant stars lying next to the line-of-sight to the limb of the sun at any given moment, if we could see them during daytime, would thus appear deflected by this much.

Einstein's General Relativity (GR), published in 1915-1916 [3,4], has had a different concept of gravity and its interaction with space and time. In GR, massive bodies curve spacetime such that light, which – contrary to the Newtonian treatment – is now massless[1] and travels in *null* geodesics, seems deflected to a distant observer. The deflection angle in this framework, as calculated by Einstein, comes out to be $\hat{\alpha} = \frac{4GM}{c^2 r}$, i.e. twice the prediction from Newtonian physics and in the case of the sun for a ray near its surface, equals to about 1".75.

In an effort led by Arthur Eddington and Astronomer Royal Frank Dyson, the deflection of light from stars behind the sun was measured during the solar eclipse of 1919 [5]. The eclipse supplied a golden opportunity to test a key prediction of the theory of General Relativity. The measurements showed that the theory was successful in predicting the bending of light in a gravitational field – the second test of GR that

[1]Be it either that light is made of zero rest-mass particles – photons, or simply a wave. It should be noted that also massive particles travel in geodesics, but not *null* geodesics, so that their deflection would be stronger, depending on their velocity.

Einstein had proposed (the first being its prediction for the precession of the perihelion of Mercury, which had already been known at the time).

Despite its critical historical role in the early days of modern physics, lensing has begun shaping as a substantial astronomical tool, observationally at least, only over the past few decades, when increasingly larger telescopes and then the HST became available.

The first observational instance of a strongly lensed, multiply imaged source was the doubly imaged quasar Q0957+561, published in 1979 [6]. Quasars are bright, quasi-stellar objects (QSOs) powered by accretion onto a supermassive black hole; they are a type of Active Galactic Nucleus (AGN). Several other multiply imaged quasars were then detected in the 1980's, including an "Einstein cross" – a quadruply imaged quasar, published in 1985 [7]. Around the same time, the first gravitational arc was observed, lensed by the massive galaxy cluster Abell 370 [8–10]. Curiously, at the time, since lensing manifestations were not yet well established, it was not immediately clear that this was a gravitational arc. A spectroscopic measurement published about a year later confirmed that indeed, the source lay behind the cluster [11,12]. This detection perhaps marks the beginning of strong-lensing science. During the 1990's, methodologies and analyses of gravitational lensing signatures by galaxy clusters started emerging, in the weak- and strong-lensing regimes [e.g. 13–17]. The spatial resolution and imaging quality afforded by the HST first with e.g. the Wide Field and Planetary Camera 2 (WFPC2) and then with later-generation instruments installed during the first decade of the 2000's – such as the Advanced Camera for Surveys (ACS) and the Wide-Field Camera 3 (WFC3) – revealed more of both the weak- and strong-lensing power of galaxy clusters and motivated the development of new lensing-analysis methods [18–25]. This recognition has sparked dedicated lensing campaigns to observe the most massive galaxy clusters and their magnified backgrounds [26–29], revealing some of the farthest known galaxies [e.g. 30,31], which supplied an additional motivation for such programs. These campaigns established that essentially every massive cluster acts as a giant strong lens in the sky – a 'cosmic telescope'. One of the deepest surveys of lensing fields was the Director's Discretionary Time program *Hubble Frontier Fields* [32], which targetted 6 massive galaxy clusters with over 800 HST orbits around earth. These observational efforts were accompanied by advancements in computational lens-modelling techniques (see section 1.3), which over the past couple of decades have reached a high level of accuracy and robustness, with greater grasp of the underlying uncertainties and systematics. In that sense, the JWST has arrived at exactly the right moment, with the lensing community already mature and prepared to exploit the new powers offered by the telescope.

In parallel to the above developments in strong-lensing science, other lensing regimes have also experienced much advancement over the past few decades. For example, various instruments, including wide-field cameras on ground-based telescopes, have been used to study weak-lensing on larger samples of clusters (e.g., [33–40]), and dedicated missions and experiments have concentrated on micro-lensing, especially towards the galactic bulge or the Magellanic clouds [41–43]. The different types of lensing are described in Section 1.2.1.

1.2. A qualitative description of lensing

Imagine a ray of light travelling through air and hitting a thin, glass convex lens such as a magnifying glass. Due to the higher speed of light in air than in glass, the ray

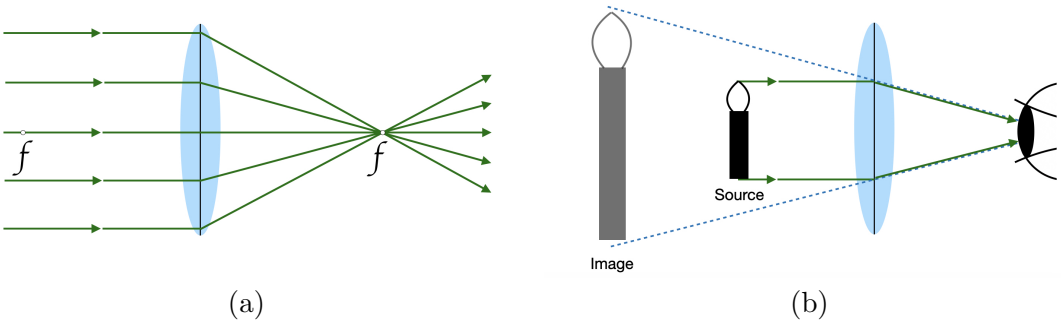


Figure 1. Qualitative description of a magnifying glass. (a) Ray diagram for a convex lens. Parallel rays are focused onto a focal point after passing through the lens, marked here on each side of the lens. (b) Demonstration of why a magnifying glass magnifies. Light rays from the source to the observer are marked with green solid lines. To the observer – the eye depicted in the figure – the rays arrive from a wider angle than that spanned by the actual source, so that the object appears larger (Note: not to scale).

would generally bend inwards when entering the glass, and then bend inwards again, when exiting the lens, and continue in that final direction unperturbed. In total, for each ray reaching the lens, depending on its position, there is an effective angle by which the ray is bent with respect to its initial direction. Parallel rays reaching the lens would be focused onto a focal point after passing through the lens (see Figure 1, panel (a)). Now assume there is a source on one side of the lens, and an observer on the other side of the lens. The lens converges towards the observer – which we can depict as a small aperture – light rays that without the lens would not reach them, thus magnifying the object. A demonstration of lens magnification is shown in Figure 1, panel (b). Light from the source (shown here as a candle but any other object would do) arrives to the observer at a wider angle than would be subtended by the source in the absence of the lens, making it appear larger. While the physics causing the effect are somewhat different hence demanding caution, we can attempt to make an analogy with gravitational lenses: Similar to the bending light ray passing from air to glass and vice versa, to a distant observer the speed of light appears reduced near a gravitating mass, implying a similar 'refraction' should occur. Thus, similarly to a magnifying glass – the lens converges light towards the observer and magnifies far away, background objects.

But there are some substantial differences between the two cases. For example, while lensing by a magnifying glass is weakly colour (i.e. wavelength) dependent, gravitational lensing in achromatic. Another important difference is that, while both cases deal with converging lenses, a simple magnifying glass deflects more strongly rays that are farther away from the lens centre (higher impact parameter), whereas in gravitational lensing the deflection usually decreases with distance from the lens' centre. This means that for the gravitational lens there is no focal point, and leads to a different image formation than in a regular magnifying glass. For example, in strong gravitational lensing images are multiplied, and while surface brightness is conserved, get highly distorted and stretched. As a matter of fact, a better resemblance to a gravitational lens is obtained by using the bottom of a wine glass, or what is sometimes called conical or axicon lenses. The glass' thickness profile causes light rays to refract in a similar way to a well-behaved gravitational lens, as demonstrated in Figure 2. Such lenses would lens a light source sitting on the optical axis, for example, into a ring. There are various examples in the literature or online of lensing analogies with

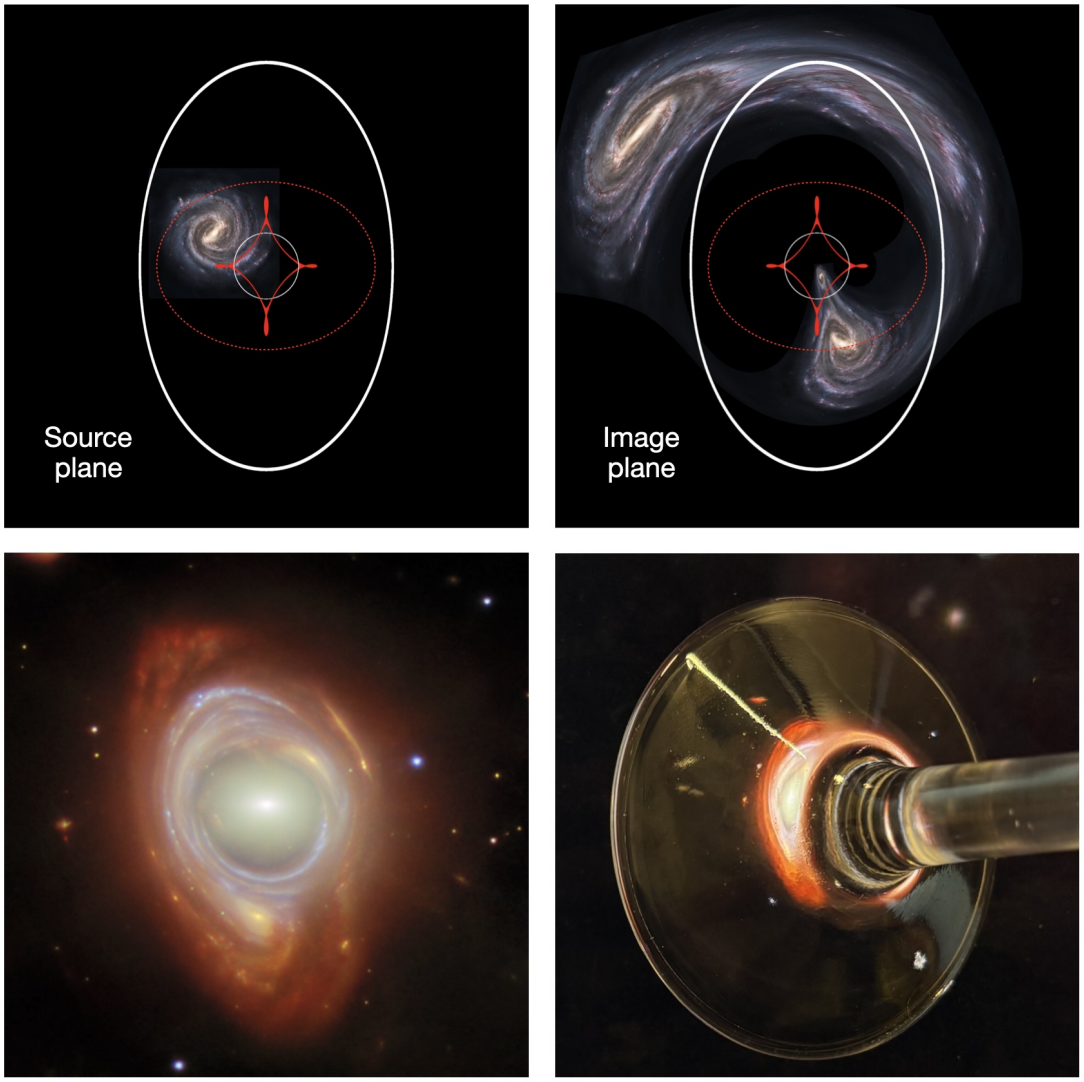


Figure 2. Examples of lensing. *Upper row:* Image formation by an elliptical lens. The critical curves of the (invisible) lens are shown in white, and their corresponding caustics in red. We plant a source between the outer and inner caustics, as seen in the subfigure on the *left*, which after lensing results in the image distribution seen in the subfigure on the *right*. Note, only parts of the source sitting within the (outer) caustic are being multiply imaged. Parts of the source sitting within the outer caustic but outside the inner one are imaged three times, whereas parts of the source galaxy sitting also within the inner caustic are imaged five times. The source-galaxy image was adopted from the web – it is an artist impression of the Milky Way based in part on NASA/ESA images (Credit: Nick Risinger). *Bottom left:* JWST image of a background galaxy lensed by a foreground elliptical galaxy, forming a wide Einstein ring. Image is from the SLICE JWST survey (Credit: ESA/Webb, NASA & CSA, G. Mahler and M.A. McDonald). *Bottom right:* Lensing through the bottom of a wine glass, using the image of the lensing-system on the left as input.

different glass lenses or with various phenomena from everyday life[2] (e.g. [44–46]).

Another analogy to everyday lenses can come from applying Fermat's principle, known from geometric optics, to the case of a gravitational lens [47–49]. If we consider all possible light rays from a source to the observer, Fermat's principle dictates that the time of arrival of a photon, given by the path integral of each ray, should be extremised (this can be thought of as a generalisation of the common notion that light takes the fastest, or shortest route). Only light rays whose path integral is stationary will thus reach the observer. Hence, one can in principle construct a time-arrival surface, whose extrema dictate where images of a certain source would form. This also means that there is a *time delay* between different images of the same source; a delay which comes in handy for various cosmological tests as we shall see soon.

Before proceeding we need to define a couple of additional terms. We mentioned that the gravitational lens has no focal point. It has however a somewhat related characteristic called *critical lines*. These lines define the symmetry points of the lens, and in principle, mark where the magnification diverges, i.e., becomes infinite. These lines, when mapped back to the source plane, are called *caustics* [50,51]. Caustics are often seen on the bottom of a swimming pool on a sunny day: The water and ripples on top of it act as an unregulated lens, focusing light rays from the sun into the observed web of caustics. In gravitational lensing, sources sitting on the caustic would be very highly magnified, where the attained magnification is limited by the source size and by the interference of light.[3] Figure 2 shows an example of the critical curves for an elliptical strong lens. Sources that sit within the caustics are multiply imaged, where the resulting configuration depends on the source position.

Finally, let us also define the *Einstein radius*. When a source is located behind the centre of a circularly symmetric lens, a ring would appear, known as the *Einstein ring*. The radius of the ring is directly related to the mass of the lens interior to the ring's angular radius, demonstrating that lensing allows us to 'weigh' astronomical objects.

More thorough coverage and useful formulae for lensing can be found in the various books and reviews about lensing already mentioned, such as [36,44,47,51,52].

1.2.1. Different regimes of lensing

Gravitational lensing can be practically divided into three regimes: strong, weak, and micro [53]. While the underlying physics is similar – namely the warping of spacetime by a massive body – the different scales involved in the different regimes make the observables, methodologies, and applications distinct.

When the projected mass density of a lens exceeds a critical density[4], as is typically the case in the centres of galaxies or massive clusters of galaxies, multiple images of the background sources appear. This is *the strong-lensing regime*, which is at the focus of this review. The mean separation between the images that form grows with the lens' mass, resulting in scales of one or a few arcseconds to a few tens of arcseconds, for galaxies and clusters of galaxies, respectively. The multiple images are typically magnified each by factors of a few to a few tens compared to the source[5], and are often

[2]The following website has a nice concentration of such examples: https://vela.astro.uliege.be/themes/extragal/gravlens/bibdat/engl/DE/didac.html

[3]The reader may notice a slight difference in terminology: In the swimming-pool scenario we referred to the caustics as the pattern forming on the observer's plane, whereas in lensing they are usually defined in the source plane.

[4]The critical density depends on the relevant distances of and between lens and source and is typically of the order of a few kilograms per square meter.

[5]Smaller sources in principle can attain even a higher magnification next to the critical curve.

also significantly distorted, stretched or sheared, sometimes merging on the critical curve such that they form giant arcs, as the first giant arc discovered behind Abell 370.

Farther away from a galaxy cluster's centre where the projected density is lower, is *the weak-lensing regime*. In that regime, background galaxies get only slightly distorted, magnified and sheared - effects that, since the intrinsic shape of each galaxy is unknown, can only be measured statistically. In the weak-lensing regime, the averaged distortions in each location can be approximated by the measured ellipticites of background galaxies. Inversion techniques can be applied, to recover – albeit with some known degeneracies – the underlying mass distribution that led to the measured shear field. This can be done both directly by inverting the data, non-parametrically, or parametrically – i.e. assuming certain parametric forms to describe the mass distribution and iterating for the best fitting result [14,35,54,55]. In the case of galaxy clusters the relevant scale to which the weak-lensing regime extends beyond the strong-lensing regime is typically arcminutes (or Mpc scales at the lens[6]). Note, also galaxies produce a weak-lensing effect around them, but given their lower mass compared to clusters and the smaller area of measurable influence they produce, analyses of the weak-lensing signal around galaxies are often done by stacking many galaxies together (e.g. [56]). Weak coherent shearing can also be produced by large-scale structure in the Universe; this is known as Cosmic Shear. Mapping the Universe using cosmic shear is an ambitious goal set by some instruments such as the Euclid space mission [57], or the Rubin Observatory [58]. As will be further mentioned below, given its excellent spatial resolution and depth, JWST is also a very useful instrument for measuring weak-lensing by galaxy clusters.

As was already established, stars cause lensing, too. Imagine looking towards the galactic bulge, where the number density of stars is high. Recall also that there are vast numbers of stars spread between us and the galactic bulge, and that stars are constantly moving in the galaxy. Occasionally, a star between us and the galactic bulge would coincide temporarily with a background star from the bulge. The relative motion of background and foreground stars results in a temporal amplification of the light from the background star. This is the *micro-lensing regime*: A star at a significant distance usually produces a lensing signal (or Einstein ring) of the order of a micro-arcsecond. Multiple images of the background star are therefore impossible to observe with current instruments, but the aggregated effect of magnification is observed, producing a typical light curve – flux as a function of time – whose properties depend on, e.g., the lensing mass, distances, and on the relative velocities. In fact, micro-lensing has also become a primary tool for detecting planets around the lensing stars, as these produce a secondary (smaller) peak on the light curve [59,60].

Some lensing scenarios can involve a mixture of the different regimes. For example, a cluster galaxy far away from the cluster's centre well in the weak-lensing regime can be chance-aligned with another background galaxy, resulting in strongly lensed images. A more scientifically important example is seen in instances of strongly lensed quasars. Since quasars are sufficiently small sources (say 10^{12} km in size), they are also prone to micro- or milli-lensing by objects in the lens such as stars, star clusters, small dark matter clumps or other substructure. What matters in determining whether a source would be susceptible to small-scale lensing is its size compared to the Einstein radius. For example, the Einstein radius of a solar-mass lens at a cosmological distance (say, billions of parsecs) strongly lensing a background source, is about 1 micro-arcsecond.

[6]A parcsec, pc, is equal to 3.086e+16 metres, or 3.26 light years.

One micro-arcsecond at the quasar's distance is indeed comparable to the size of its emitting region. The effect is seen when comparing the light curves of the quasar's multiple images, where each light curve shows additional fluctuations not observed in the other images. Larger or more massive substructure in the lens can also cause longer-term *flux ratio anomalies*.

1.3. Strong-lens modelling

It should become insightful to understand how lens modelling is carried out in practice. By 'lens modelling' we refer to constructing a model for the projected mass distribution of the lens. The potential, deflection angle, Fermat surface, and other relevant quantities all consistently relate to that mass distribution. Although the constraints we have are mainly from the positions of multiple images, i.e., on the deflection angle directly, it is often easier to model the potential, and from it to derive all other properties (deflection angle, mass distribution, etc.). I also remind the reader that we are concentrating here on strong lensing by galaxy clusters. In the case of galaxy-scale lenses, only one source typically, but sometimes two or three sources are seen lensed, forming multiple images around the galaxy and the symmetry is usually simple and clear (this however does not mean that obtaining a very precise solution is an easy task!). In contrast, galaxy clusters are much more complex bodies and can have many dozens, sometimes hundreds, of multiple images spread across their field.

Our first mission when modelling a galaxy cluster strong-lens then is to identify the families of multiple images of the different background sources. The idea is to use the lens equation, which maps an image to the source plane, while remembering that all images of a certain source should trace back to the same source position. Although the trained eye can often associate a substantial part of the families based on symmetry and colour information, the identification often involves photometric or spectroscopic *redshift* measurements, as well as an iterative process using the lens model under construction. *Redshift*, denoted hereafter by z, defines the factor $(1+z)$ by which the Universe has expanded since the observed light left the source. Generally, it is also a measure of distance: The higher the redshift, the larger the distance. Since the universe expands, objects farther away from us – whose light also took longer to get to us – are *redshifted*. Photons emitted at a certain wavelength from a source at redshift z will be received by us at a wavelength longer by a factor $\times(1+z)$. In practice, the redshift of a source can be measured spectroscopically, by comparing the observed and rest-frame wavelengths of known emission lines; or photometrically, by probing from a range of spectral templates which redshift and template best produce the observed broadband colours. Redshifts are important not only for associating multiple images, but also because they translate into the relevant distances needed for pinning down the lens model. For multiply imaged sources that do not have a spectroscopic measurement, a photometric redshift can be assigned, or alternatively, their redshift can be left free as one of the parameters of the model.

Assuming at least some multiple images families have been identified, we can now construct a first model[7]. The basic idea, which is similar in nearly all methods, is to decide on a manner to describe the mass distribution, or on a set of assumptions, and then iterate on many realisations of the mass distribution under those assumptions, searching for the one that reproduces best the observations. For example, 'free-form'

[7]There are in fact methods, such as Light-Traces-Mass [20,62] that are useful for the detection of multiple-image families following an initial well-guessed mass distribution.

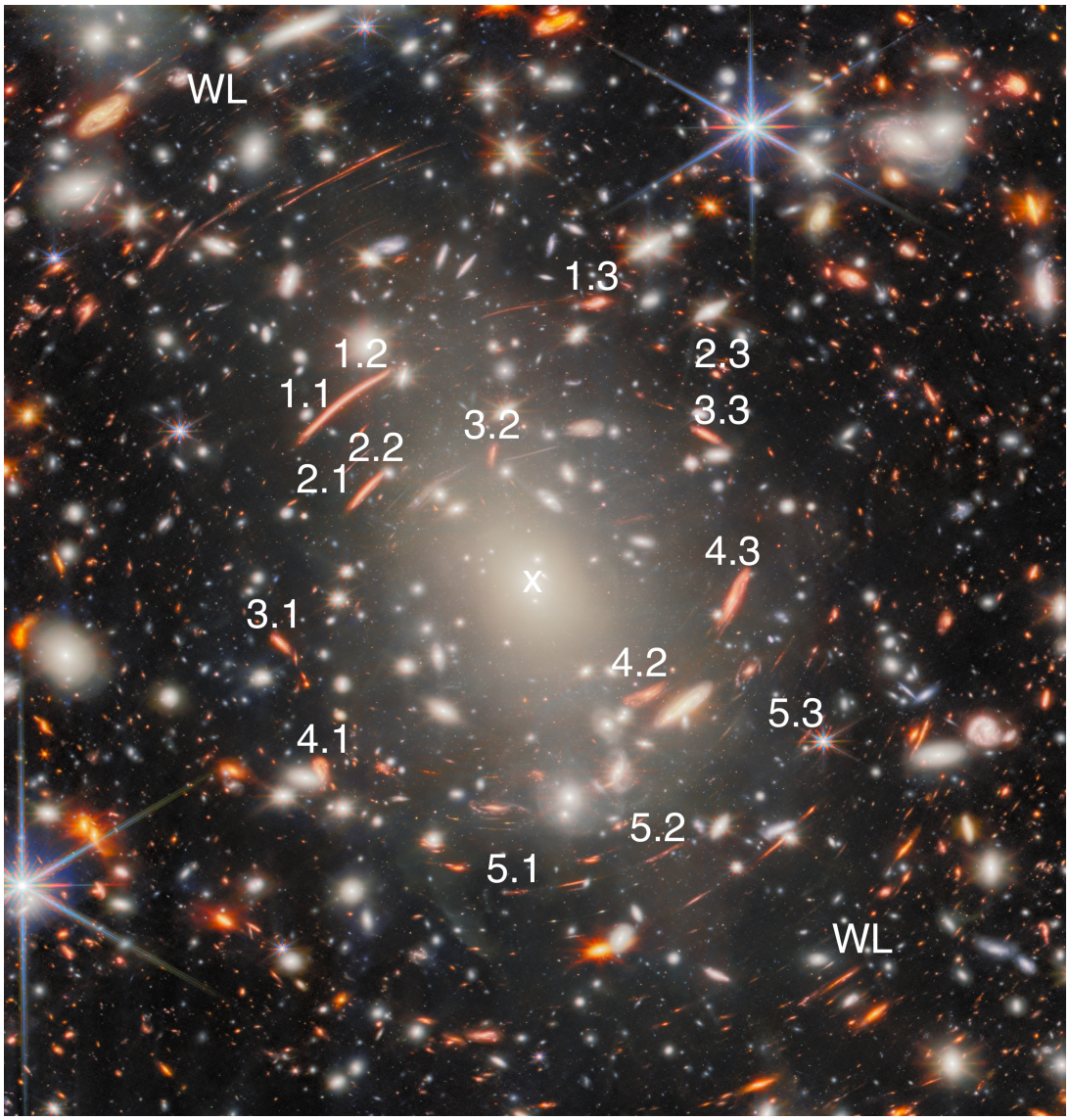


Figure 3. One of the deepest fields imaged with JWST/NIRCam to date, the lensing cluster AS1063. Image was taken as part of the GLIMPSE survey [61], reaching about 31 AB magnitudes per band before accounting for lensing magnification. In the centre of the image lies the brightest cluster galaxy, marked with an "X", sitting at the heart of the cluster's potential well and thus lensing centre. Around it are seen multiple images of strongly lensed background sources, some of which are indexed with a different leading number per family. Outwards beyond the strong-lensing regime, singly lensed tangentially sheared arcs are seen, where the weak-lensing regime roughly commences (marked with "WL"). Credit: ESA/Webb, NASA & CSA, H. Atek, M. Zamani (ESA/Webb), R. Endsley.

methods [24,63,64] might assume that the larger-scale mass distribution can be modelled as a combination of some basis functions such as pixels or Gaussians, and are thus not limited to a certain pre-determined overall form [65]. Parametric techniques, in contrast [22,66,67], typically assume a pre-determined functional form for cluster galaxies, which are needed for an accurate reproduction of multiple images, and a large-scale functional form to represent the dark matter distribution (which is assumed to dominate the mass budget), and then iterate on the values of the parameters of these functions until the solution which best reproduces the observables (i.e. multiple im-

ages) is found. Typically, only the positions of multiple images are being used, but it is also possible to use the shape and surface-brightness distribution, magnification ratios, or time delays (see e.g. Table 1 in [68]). The optimisation, i.e., minimisation of a cost function (typically χ^2) quantifying the distance between observed and predicted multiple images, and exploration of the relevant parameter space can be done either via a grid, or more efficient methods such as gradient descent or Markov Chain Monte-Carlo. The typical accuracy for cluster lens models is of the order of a few tenths of an arcsecond. Such deviations are expected due e.g., to matter along the light-of-sight that is not independently modelled [69], or outliers in the several scaling relations assumed [70] – for example, in the scaling relations which determine the mass and extent of galaxies based on their luminosities. Thus contemporary lens modelling software is already capable of producing very high-fidelity results of the cluster's mass distribution. Such results have been vetted by examining the methodologies on a set of numerically simulated clusters, as well as by confronting their predictions for time delays and magnifications of lensed supernovae with observations and simulations [71,72]. These tests have been imperative in the efforts to compare and improve high-end lens modelling techniques.

2. 'Classical' applications of strong lensing

We mentioned that over the past 2-3 decades lensing has become an important tool in astronomy. However, we did not yet explain to what end. Since we have a 'cosmic lens' or a 'looking glass' in the sky, it distorts and magnifies background objects that lie behind it. Hence, one immediate application of strong-lensing is that it allows us to study far-away galaxies in greater detail, as well as to observe faint and distant galaxies that without lensing may be too faint to be observed. Indeed, this advantage has led to cluster-lensing campaigns with the HST, constantly supplying record-breaking, high-redshift (and thus early) galaxies, thanks to lensing [18,30,31,73–77].

In terms of numbers, however, it should not be obvious that lensing is advantageous for studying high-redshift galaxies. First, some other, record-breaking high-redshift galaxies have been detected also without the aid of lensing (mostly brighter ones; e.g., [78–81]). Second, while lensing magnifies the background behind the lens and thus pushes more objects above the detection limit, since surface brightness has to be conserved, lensing effectively probes a smaller area in the source plane, per given field-of-view of a telescope. In terms of numbers, this trade-off between higher magnification and reduced source-plane area becomes advantageous only if the high-redshift luminosity function – the density of galaxies per luminosity and redshift bin (see also section 3.1.1) – is sufficiently steep [82]. Indeed, thanks to lensing campaigns, it was established that the luminosity function was in fact as steep [e.g. 83,84]. But regardless of the slope or net gain, lensing is in any case beneficial – and maybe the only way – for uncovering objects that would otherwise be simply too faint to be observed.

Another advantage from strong lensing for high-redshift galaxies comes from image multiplicity. The deflection angle of an image scales as the ratio of the distance between lens and source and the distance to the source. This ratio saturates for high-redshift sources as the two distances grow more similar, but it is very useful for discriminating between lower-redshift and higher-redshift sources: Since the deflection depends on source redshift, the lens size or area within the critical curves increases for more distant, higher-redshift sources, increasing the angular separations between multiple images. Because most high-redshift galaxies have been identified photometrically based

on their colours [30,77], this 'nesting effect' could thus be used as a decisive, reinforcing evidence for the high-z nature of the candidates [31,76]. This was particularly useful in the era prior to JWST, when obtaining spectra for high-redshift candidates was mostly limited to observations from the ground, and was thus extremely challenging and often impossible.

In order to analyse the lensed backgrounds we must construct a lens model, so we can obtain, for example, an estimate for the magnification by which background objects are magnified. The lens model essentially defines a mass distribution for the lens. Since most of the matter in the Universe, particularly in massive objects such as galaxy clusters, is believed to be dominated by an unseen component dubbed *dark matter*, we thus have a means for mapping the unseen. Hence, a second immediate feat from lensing is the ability to map cosmic structures, and in particular the distribution of the otherwise-invisible dark matter. Such efforts are crucial for our understanding of dark matter, which continues to be one of astronomy's – and in fact physics' – greatest mysteries. Some unique examples, such as the Bullet Cluster [85–87] which exhibits an offset between dark matter – probed by lensing and coincident with the galaxies – and the gas lagging behind, imply that the dark matter self-interaction cross section is very small, consistent with zero (i.e. dark matter is referred to as collisionless). Furthermore, comparing properties of the resulting mass maps to analytical models or numerical simulations teaches us about dark matter, structure formation, and our physical universe through various cosmological parameters [88]. In addition, galaxy clusters, being the most massive gravitationally bound objects in the universe, are great laboratories for studying various astrophysical processes such as gas physics and dynamics. Coupling the gravitational potential inferred from lensing with a range of other observables such as X-ray or the Sunyaev-Zel'dovich effect teaches us about cluster physics and can also enable 3D mapping of the clusters [89,90].

Lensing also supplies additional probes of cosmology. The time delay between multiple images depends on the distances of and between the lens and source. The relevant combination of distances is often called the time-delay distance, providing an absolute distance scale which is inversely proportional to the Hubble constant, H_0. The observed time delay of multiply imaged variable sources such as quasars, combined with a lens model and redshift measurement, thus constitutes one of the few principal means to measure the expansion rate of the Universe [91,92]. As such, it has been of great importance adding to the 'Hubble tension' between low-redshift distance ladder measurements of the Hubble constant [93,94] and those obtained by *Planck* observations of the *Cosmic Microwave Background* [95]. In other instances, since lensing distances of background sources depend on the cosmological parameters such as matter density and on the dark energy equation of state, their ratios can be used to constrain these parameters [96].

In summary, then, the main scientific themes that have been typically studied with lensing are dark matter, cosmology, and distant or high-redshift galaxies. Observations with the HST over the past few decades allowed for sufficiently high resolution data to realise these objectives and push these fields to previously unimaginable frontiers, revealing, for example in the high-redshift regime, galaxies as early as 500 Myr after the Big Bang.

3. Strong lensing with JWST: A new era

A major leap in strong-lensing science followed the advent of JWST. After more than 20 years in development and much anticipation by the astronomical community and science aficionados alike, the JWST was launched into space on Dec 25th 2021. With an effective mirror size of 6.5m in diameter, JWST is the largest telescope in space. It operates in a wide wavelength range from red-optical to the mid-infrared (0.6–28 μm, roughly), with four advanced instruments for imaging and spectroscopy. Its size and wavelength coverage supply unprecedented sensitivity and resolution; it can reach to $\sim$30 AB magnitudes[8] in a reasonable exposure time, with a spatial resolution (FWHM) of better than $0.03''$ at short wavelengths, and $0.07''$ around 2 μm. The observatory is thus ideal for studying distant sources – whose UV and optical light, due to the expansion of the Universe, is redshifted towards longer wavelengths. Indeed, a primary goal of the JWST is to study the first stars and galaxies – 'first light'.

3.1. High-redshift galaxies with JWST: An uncharted territory

3.1.1. The UV luminosity function and reionisation of the Universe

It has been well established that the inter-galactic Hydrogen was reionised during the first billion years of the Universe. One of the long standing questions regarding this important process, was whether galaxies drove reionisation thanks to UV radiation from massive stars, or whether it was AGN or other exotic sources that supplied the required radiation field. The key to answering this question is the number of galaxies and their ionising contribution. The 'counting' of galaxies in different wavelengths and luminosity bins forms what is known as the *luminosity function*, whose shape and evolution are thus of great interest, as they help us characterise the shape and timeline of reionisation. Because there are far more fainter galaxies than brighter ones, lensing – which can typically push observational limits for detecting distant galaxies by several magnitudes – is bound to play a critical role in probing the faint and distant population in the early universe.

A common functional form used to describe the luminosity function is the *Schechter function* [108]. It comprises of a power-law with slope α on the faint end, and an exponential cutoff towards the brighter end where fewer galaxies are expected, beyond a characteristic luminosity L^* (or absolute magnitude M^*). The normalisation of the function is given by Φ^*. See for example Fig. 4.

Prior to JWST, pairing deep HST observations with lensing fields such as the Hubble Frontier Fields clusters allowed astronomers to construct robust, high-redshift luminosity functions to an ultraviolet absolute magnitude as faint as $M_{UV} \sim -15$ [9] towards $z \sim 8$ [83,109], hinting that galaxies were indeed, likely responsible for reionisation; in particular, if the slope of the luminosity function continued unchanged to fainter magnitudes [110]. But given this regime was largely unreachable with *Hubble*, it was not clear whether this was indeed the case [83,111]. Some early programs with JWST, such as GLASS-JWST [112], the CAnadian NIRISS Unbiased Cluster Sur-

[8] Astronomers often express flux densities on a logarithmic scale called magnitudes. The AB magnitude system, for example, is defined as $m = -2.5\log_{10}(f_\nu) - 48.60$, where the flux density f_ν is in units of erg s^{-1} cm^{-2} Hz^{-1}.

[9] M_{UV} refers to the *absolute magnitude* (in the ultra-violet, in this case), defined as the apparent magnitude of the galaxy, m, were it placed 10 parsecs away, $M \approx m - 5\log_{10}(\frac{d}{10})$, with d the distance to the galaxy, in parsecs. $M_{UV} \sim -15$ at $z \sim 7-8$ corresponds to an apparent magnitude of about $32-33$ AB.

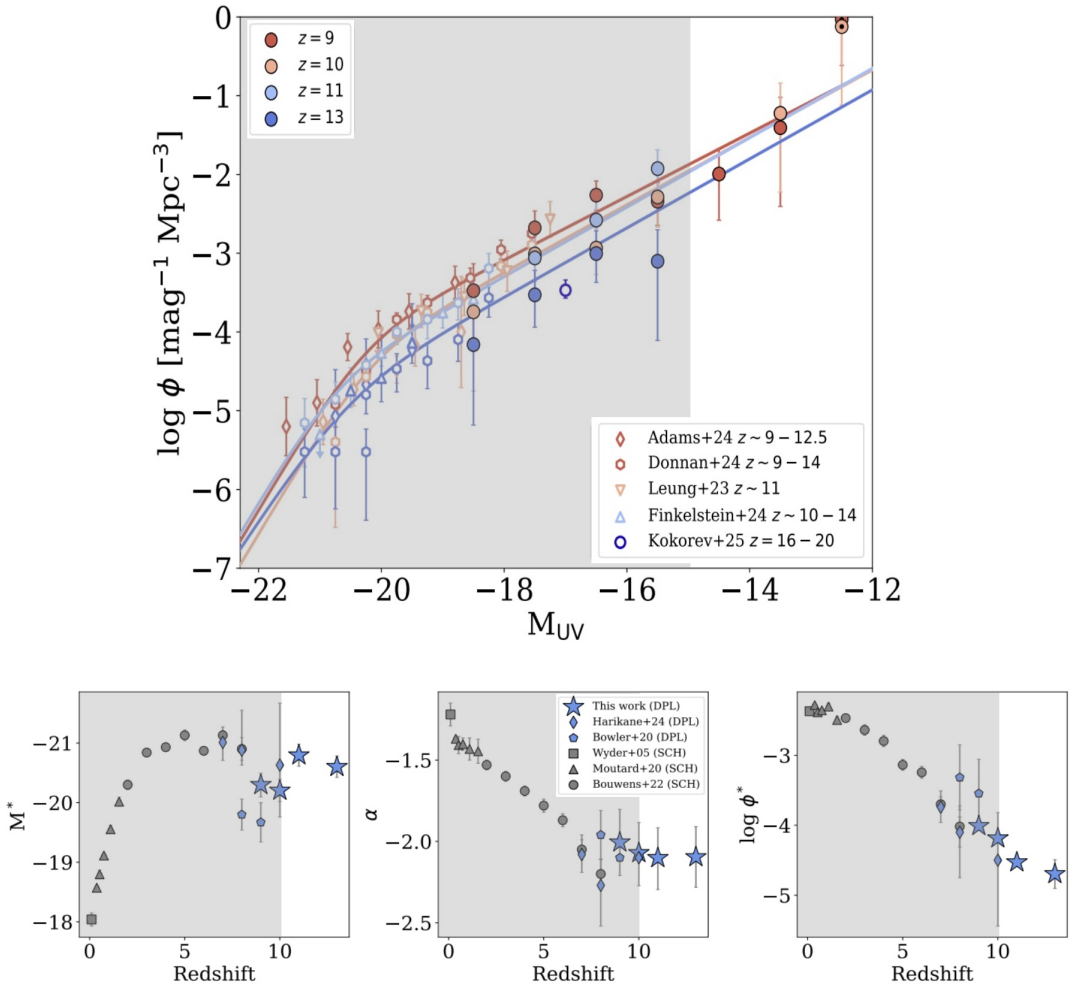


Figure 4. Deep view of the faint end of the luminosity function allowed by JWST+Lensing. The upper subfigure shows the luminosity function derived from very-deep observations of the lensing cluster AS1063 taken for the JWST/GLIMPSE program (seen in Figure 3) [97], compared to several other works from the literature [98–102]. The bottom panels show the evolution of the luminosity function parameters with redshift, also compared to various works [103–107]. Note also the steepening of the faint-end slope α at high-redshift, making lensing particularly beneficial. I overplot here, on the figures adapted from [97], the limits reachable with HST as shaded grey regions, taken here nominally as M_{UV}=-15 (at $z \sim 8$), and $z = 10$. As can be seen, the combination of JWST with lensing enables us to improve the constraints and probe far beyond these limits, to very faint and distant galaxies inaccessible otherwise.

vey (CANUCS, [113,114]), Prime Extragalactic Areas for Reionization and Lensing Science (PEARLS, [115]), and Ultradeep NIRSpec and NIRCam Observations before the Epoch of Reionization (UNCOVER, [116]), extended this previous success and targetted lensing fields to push observational limits deeper than ever before. Some of these programs reached already imaging depths of $\sim 29-30$ magnitudes per band before additional $\sim 2-3$ magnitudes from lensing, finding for example – among many other important results – that galaxies were likely responsible for reionisation [117]. The gravitational lensing & NIRCam imaging to probe early galaxy formation and sources of reionisation (GLIMPSE, [61]) program, which observed with JWST one of the Hubble Frontier Fields clusters, AS1063, for 20-40 hours per band reaching 31 AB magnitudes before accounting for further boost from lensing, supplies one of the

deepest fields ever imaged (Fig. 3) and pushes the limits towards $M_{UV} \sim -12$, marking a major advancement over the limits reached with *Hubble* and enabling better insight into the drivers of reionisation unachievable without the aid from lensing. The luminosity function from this survey is shown in Fig. 4. This additional insight also includes lensed galaxies exhibiting potential signatures of population III stars - the first generation of stars that was formed in the Universe [118]. The ongoing program Vast Exploration for Nascent Unexplored Sources (VENUS, e.g. [119]) is targetting a large number of clusters, which should both help to overcome cosmic variance and allow for substantial areas of high magnification, thus probing the $M_{UV} \simeq -12$ regime at $z \sim 6$–9 as well.

3.1.2. The most distant galaxies in the Universe

The ability of JWST to observe fainter and farther than ever before naturally revealed new, record-breaking galaxies. Its spectroscopic capabilities now also allow us to confirm their redshifts, through emission lines or through their spectral break near the Lyman limit. While *Hubble* could only observe galaxies out to redshift $\sim 11 - 12$ [31,78,80], at the time of writing there are already several galaxies spectroscopically confirmed with JWST around redshift $\sim 14 - 14.5$ [120–122] (see also Fig. 5 here), and some photometrically selected galaxies up to higher redshifts [123]. Interestingly, although $z \sim 12 - 13$ galaxies have already been spectroscopically detected behind lensing clusters (e.g. [124–126]), currently the 2-3 farthest galaxies at $z \sim 14$ are relatively bright field galaxies chosen from wider field surveys with JWST, and not strongly lensed galaxies. This may be regarded as somewhat surprising since with *Hubble*, individual, high-redshift lensed sources seemed to have been more prominent (e.g. [31,76,127]), although the two farthest galaxies detected with *Hubble*, GNz11 [80] or UDFj-39546284 [78,128,129] are also bright field galaxies. We may thus expect that new record-breaking galaxies will also be discovered behind lensing clusters soon, but this prediction depends on various factors such as the shape of the luminosity function, contamination from intra-cluster light, and how JWST resources are divided between field surveys and cluster lensing programs. Note, lensed candidates have also been detected to redshift 16 and beyond [102], albeit currently lacking spectroscopy.

3.2. Strongly lensed Active Galactic Nuclei and Supermassive Black Holes

Multiply imaged quasars and AGN have long been of great interest. They can be used to measure the expansion rate of the Universe through time delays [92,131], substructure in the lens through flux anomalies [132], the size of the source through micro- or small-scale lensing [133], or its mass through changes in brightness (and their echo from outer regions; a technique known as *reverberation mapping*), which can be monitored more effectively thanks to lensing time delays [134,135]. Nevertheless, while many dozens of lensed quasars have been found to date, and many more are expected now with new large sky surveys such as Euclid, Roman, and Rubin/LSST, most of those are lensed by galaxies. Only several multiply imaged quasars have been found behind clusters to date (e.g. [136–144]).

It has been shown that bright, strongly lensed objects that maintain a point-like morphology may suggest an underlying supermassive black hole [145]. Although JWST has been active for only four years, a few other multiply imaged AGN candidates have already been found following this rationale [146,147]. Thanks to its increased resolution and depth, it can be assumed that additional multiply imaged AGN will be similarly found with JWST soon. Another benefit from lensing comes from the magnification, which allows us to study smaller-mass black holes. Lensing surveys of large numbers of clusters with JWST such as the VENUS program, can now measure black hole masses down to $\sim 10^5$ solar masses in lensed galaxies and shed light on their co-evolution with their host galaxies through cosmic history.

In its first year of operations JWST detected an abundance of faint AGN at high redshifts [148,149], with lensing supplying some additional, unexpected finds. In one of the first, deep cluster fields observed with JWST, Abell 2744, imaged for UNCOVER program, a puzzling source was discovered: A triply imaged, $z \sim 7$ *extremely red and compact* source ([146]; see Figure 6 here). The source, despite being magnified and sheared by lensing, remained a point source across its three images, thus implying a size of less than ~ 30 pc. Given its clear quasi-stellar appearance in JWST data it was given the name Abell2744-QSO1. It turned out this source had originally been found with

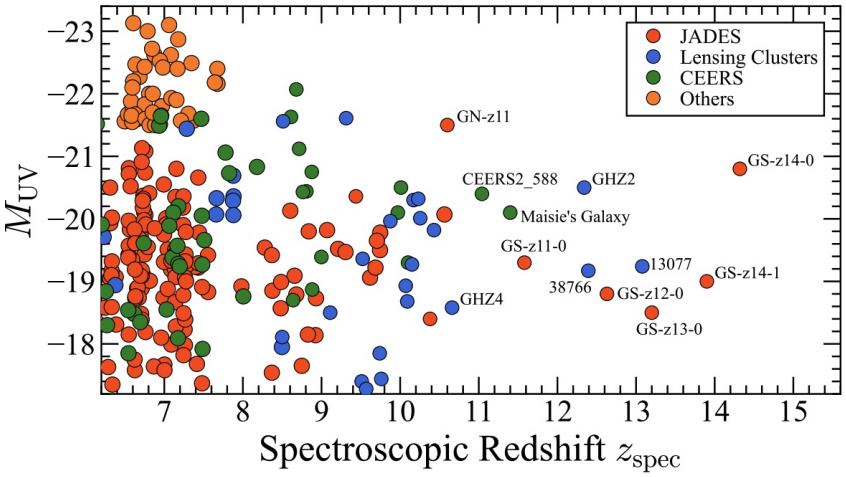


Figure 5. Compilation of high-redshift galaxies from the literature. Figure is taken from [130]; see references therein. Note the prominent contribution of lensing to high-redshift galaxy detection and the numerous galaxies now detected and spectroscopically confirmed with JWST beyond the limits allowed by HST ($z \sim 11$).

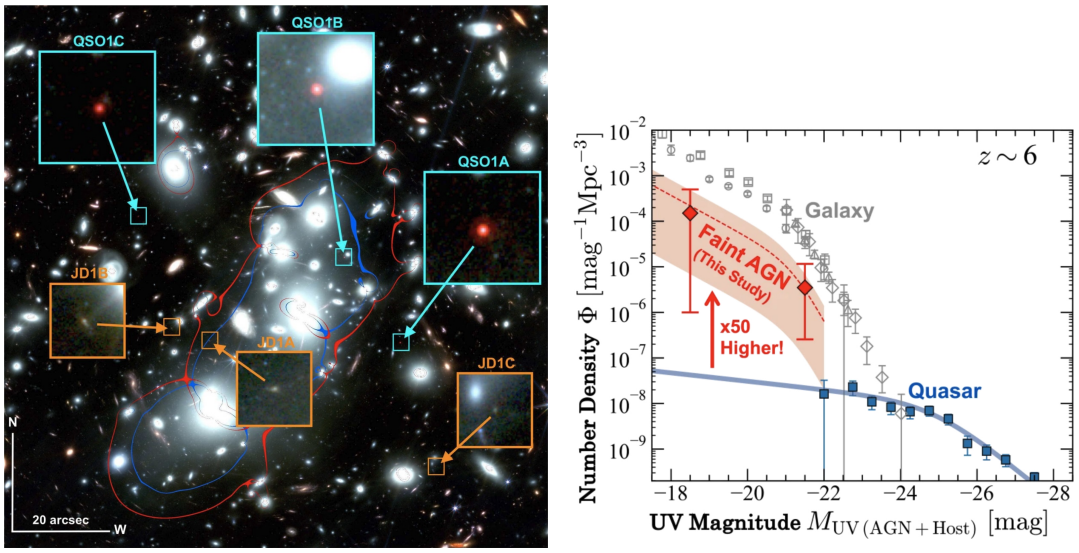


Figure 6. JWST revealed an unexpected population of faint AGN. Left: Image of the lensing cluster Abell 2744 taken as part of the UNCOVER JWST survey (Credit: NASA, ESA, CSA, I. Labbe, R. Bezanson, L. Furtak, A. Zitrin; figure from [146]). A distinct, triply imaged red and compact source was detected, labelled QSO1. Despite large magnification and shear, it remained a point source over its three images suggesting a very small source size. Another high-redshift triply imaged galaxy, JD1, is highlighted for comparison. A2744-QSO1 became a proto-type of a population now known as LRDs. Together with its unique V-shaped SED, this suggested that LRDs could be powered by SMBH [152]. Right: The population of faint AGN discovered by JWST is ×50 more abundant than extrapolations from previous, brighter quasars. Figure from [157] (see also references therein). Lensing helps push the luminosity function fainter by about 2 additional magnitudes [158].

Hubble as a $z \sim 7$ candidate [150], but *Hubble* lacked the resolution and wavelength coverage needed to reveal its uniqueness. Spectral energy distribution (SED) modelling using the extended wavelength coverage allowed by JWST suggested a high mass, similar to other, over-massive red objects previously reported by e.g. [151]. But now, thanks to the size constraint from lensing, it was obvious that it would be difficult to have so many stars packed in such a small region; the density would be unreasonably high. The most obvious explanation was, similar to brighter quasars or AGN, that the radiation was due to accretion onto a SMBH. Indeed, follow-up observations revealed broad Balmer-series emission lines of several thousand km/s widths, indicative of AGN, and further revealing a high black-hole to host mass ratio [152]. But the object had a couple of other distinct features which were not typical of broad-line AGN: It had a blue UV spectral slope but red optical slope, forming a unique V-shape SED, and it lacked X-ray or radio detections, motivating also other alternative explanations. Several other such red and compact objects were quickly detected around the same time, in the field or more modestly magnified regions, and were given the appropriate name *Little Red Dots* [153–155]. Many dozens of LRDs have been by now detected across various JWST fields at a range of redshifts [156].

Abell2744-QSO1 continued to play a pivotal role in understanding LRDs. Since there exists a substantial time delay between the images, it is possible to search for variability – an expected signature of Type I AGN – among the three images of QSO1, which effectively span about 20 years of observations. Signs for variability were found in the strengths (or equivalent widths) of broad Balmer line emission from QSO1 [160,161], supporting the AGN scenario.

Lensing also enables another important measurement for AGN: For the high mag-

nifications typically seen for strongly lensed sources, and for high enough black hole masses, the sphere of influence of the BH becomes observable with JWST (e.g. [162]). NIRSpec/IFU observations supplied such direct dynamical mass measurement also for Abell2744-QSO1 [159] (see Fig. 7 here).

A few more multiply imaged LRDs have been by now discovered in recent lensing campaigns [163,164]. Some of these show additional detail such as a close-by blue emission [164,165] or a LRD close pair [166], thanks to lensing magnification (see Fig. 8). Investigations of the nature of some of these companions are ongoing.

3.3. A magnified view of distant galaxies

The high magnification from lensing coupled with JWST allows us to obtain a more detailed view of distant galaxies than was previously possible, reaching a spatial resolution of about a few tens of pc in the source plane. *Hubble*, coupled with lensing, supplied a magnified view of distant galaxies in some representative cases going down to 50-100 pc resolutions at redshifts $\sim 2-5$, for example [169,170]. With JWST, this enhancement is further boosted and these numbers can be improved by factors of a few per object, simply given the ratio in mirror diameters. Together with the extended wavelength coverage, this also allows us to observe different types of galaxies in detail to higher redshifts. For example, spiral galaxies at increasing redshifts have long attracted attention, as these can shed light on when and how these spiral structures formed (e.g. [171]). The JWST, with its increased resolution now enables us to observe spiral galaxies to higher redshifts than before and indeed, various samples up to at least $z \sim 5$ have been assembled [172–174]. Such galaxies could be seen with even further detail, were they lensed. For example, Figure 9 shows a clear spiral structure in some distant galaxies, including a couple of lensed ones, at redshifts $z \sim 3-4$.

3.4. Star clusters

Understanding star formation and galaxy evolution across cosmic history is one of the key goals of modern astronomy. As fundamental building-blocks of galaxies and an excellent tracer of their star formation history [178–181], star clusters are thus of

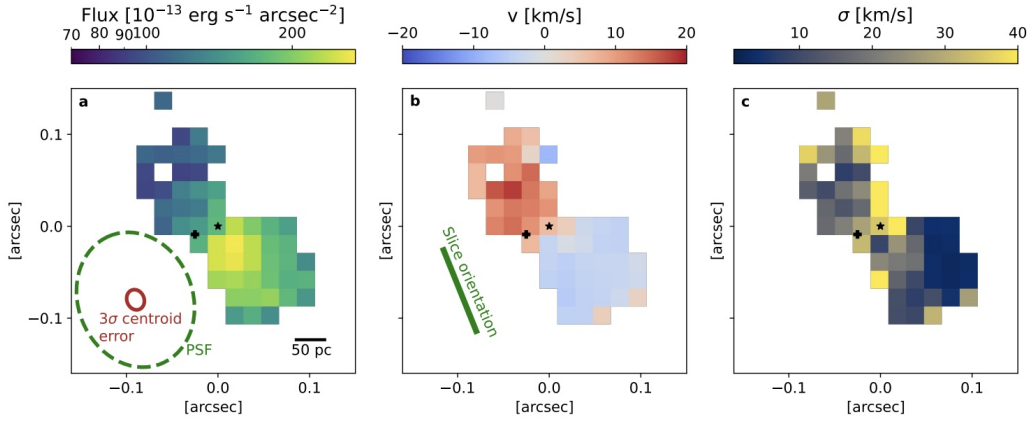


Figure 7. JWST allows to resolve the sphere of influence around strongly magnified SMBHs in the early universe, enabling a direct dynamical mass measurement. The Figure, taken from [159], shows the Hα flux, velocity, and velocity dispersion fields around A2744-QSO1 using NIRSpec integral field observations.

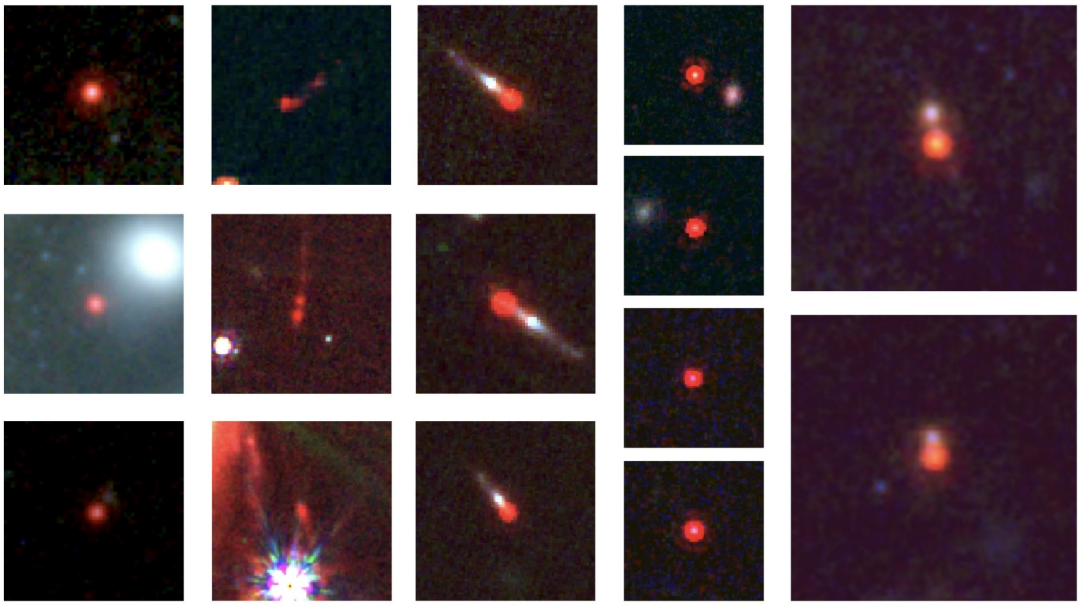


Figure 8. Compilation of strongly lensed LRDs. Each column shows a different system of a multiply imaged LRD (see [146,164,165,167,168]). The stamps were constructed here from public data and their sizes arbitrary. As can be seen, LRDs maintain a point-like appearance despite significant magnification, which places strong constraints on their physical size. Some of the LRDs have also a notable, nearby companion.

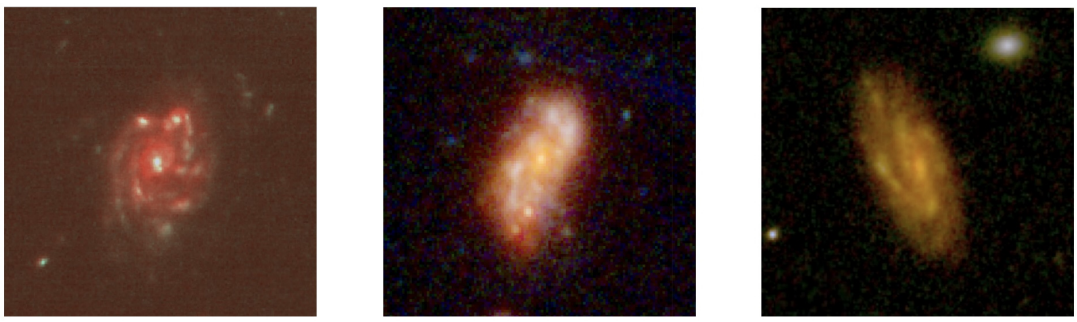


Figure 9. JWST observes disk and spiral galaxies farther than ever before. From left to right, the subfigures show the Big Wheel galaxy at $z = 3.25$ ([175]; not gravitationally lensed); galaxy Alaknanda, at $z \simeq 4$ ([176]; moderately gravitationally magnified by the galaxy cluster Abell 2744); galaxy Charybdis at $z \sim 3.6$ – an apparently spiral galaxy strongly lensed and triply imaged by the galaxy cluster MACS J1931.8-2635, enabling the detailed view [177]. Stamps are constructed from public data and their orientations and sizes are arbitrary.



Figure 10. Collage of star-forming clumps, globular clusters, and highly magnified arcs seen with JWST throughout cosmic history. Shown here are example arcs and clumps up to redshift $z \sim 11$ complied from the literature [119,182–188] or from various lensing surveys [61,115,116], and constructed here from publicly available data (Credit: ESA/Webb, NASA & CSA). Many of these clumps and point sources could not be resolved prior to JWST. Especially in highly magnified arcs, these are now resolved down to $\sim$ 1 pc. The orientations and stamp sizes are arbitrary.

great interest. Their formation and evolution, feedback mechanisms and effects on the interstellar medium, as well as the survival mechanism of gravitationally bound clusters through redshift, have been largely unknown. Indeed, directly observing star clusters beyond the low-redshift universe has been very challenging: Even young star clusters with orders of 10^5 stars remain faint ($>$ 29 AB in the blue [180]), and with physical scales of $\sim$pc to couple dozen pc they remained largely unresolved (for example, a 20 pc object at redshift 1 occupies an angular size of a few 0.001 arcseconds).

One of the first images by JWST that was released to the public was of a galaxy cluster lens, SMACS J0723.3–7327, revealing an unprecedented amount of detail and specifically, many previously unobserved point sources; either star clusters in the intracluster light, or lensed star clusters in the background, for example in or around the halos of magnified distant galaxies. The first striking example for this was likely the Sparkler galaxy [182], seen lensed by the cluster (upper-left stamp in Figure 10 here). The JWST image of the galaxy revealed various star clusters surrounding it; objects we could simply not see before. Various similar galaxies have been detected since with JWST (see Figure 10), suggesting that, when combined with lensing, JWST allows us to study star formation at the smallest scales.

But it is also JWST's wavelength coverage that plays a role in pushing the limits, enabling stellar population synthesis in star clusters at growing redshifts. In that

respect it is worth noting that JWST has managed to study several gravitational arcs at high redshifts [185,187]. To form a gravitational arc the source has to sit on the caustic, and this scenario is thus rarer. But this configuration is interesting in another aspect, too: A source sitting on the caustic would be significantly stretched and some parts of it very highly magnified. The turn-over in angular-diameter distance towards high-redshifts[10] aids in increasing the probed physical resolution as well. Indeed, JWST enabled the detection of star clusters as small as 1 pc, revealing when, where, and how the first stellar populations and proto–globular clusters formed. At high redshifts these may also be the sites from which ionising radiation is coming, and is thus important also for understanding the role of early galaxies in reionisation.

3.5. Lensing of stars at cosmological distances

Lensing of distant stars marks a remarkable advancement in strong-lensing science over the past decade. In the previous subsection we mentioned that a gravitational arc forms when the source – typically a galaxy – sits on the caustic, and some parts of it get highly magnified. Because objects move in space, there is a relative transverse motion between the source, lens and observer, so that effectively, the source moves transversely with respect to the line-of-sight to the lens. Stars in that source galaxy will thus occasionally sweep across the caustic, and get extremely magnified as they do – producing a typical light curve, as was already predicted three and a half decades ago [189]. The maximum magnification that a source can attain is limited by the size of the source and thus, for stars, can in principle reach even $\sim 10^5 - 10^6$. This means that *individual stars* at cosmological distances can be temporarily observed with lensing. These events are often called *caustic crossing events*. The caustic crossing time, given by the star's radius divided by the velocity (say, hundreds of km/s), is of timescale of hours to days, typically.

The first instance of an extremely magnified star crossing the caustic of a cluster lens was serendipitously found with the HST already a decade ago, when monitoring the galaxy cluster MACS J1149.5+2223 [190]. Once it was realised that *Hubble* could see individual stars, an effort was made to characterise such events: What type of stars or other sources (for example pristine population III stars and their stellar-mass black hole accretion disks [191]) are more likely to be found, the expected rate, or dependency on various parameters such as microlens density [192–194] or Initial Mass Function [195,196] – the distribution of masses of newly born stars. In parallel, more events of lensed stars were found in different clusters [197–199], in random or dedicated lensing campaigns. Some systematic searches supplied important empirical limits suggesting that although CCEs can be seen with *Hubble*, the rate of events is quite low simply because typical HST observations are not deep enough [200]. The first event in MACS J1149.5+2223, it turned out, was at the relatively bright end of the expected distribution of events.

The first caustic-crossing events supplied another important insight. In practice, the lens itself is also composed of stars and other massive substructure. This means that the (macro) caustic is surrounded by smaller micro-caustics, or that it is not smooth, but breaks into a net of smaller micro-caustics [192,193]. In fact, the amount

[10]The angular-diameter distance is a cosmological distance measure defined as the ratio of an object's physical size to its observed angular size. The angular-diameter distance increases with redshift since more distant sources appear smaller on the sky, but at some point turns over and decreases with source redshift. This is because in an expanding universe, very distant sources were much closer to us when they emitted the light that is now reaching us.

of micro-lensing can also teach us about the composition of the lens and thus also important for studying the stellar population and compact dark matter content in the lens. Correspondingly, the light-curve during a caustic-crossing event, as was seen in MACS J1149.5+2223 [190], would break into multiple smaller peaks, each typically with magnification of 'only' a few hundreds to a few thousands. This, nonetheless, is still sufficient to observe single stars close to the caustic [201]. Bright, super-giant stars can be naturally observed as (micro-)caustic crossing transients also somewhat farther away from the caustic (even up to about ~ 1 arcsecond or more; [202]). Very close to the position of the macro-caustic, when in the net, stars will appear semi persistent – they can remain highly magnified for decades – showing only minor flux fluctuations. Earendel, the highest-redshift star candidate to date [203,204], is one of those cases, and thus in principle can also be a star cluster [205].

While Earendel was originally detected with HST, early results from the first year of JWST operations already revealed a couple of other high redshift $z \sim 5$ stars [207] (Fig. 11, upper panel). Remarkably, follow-up observations with NIRSpec captured the spectrum of one of the stars [206] (see Fig. 12 here). The spectrum fitted well the expectations from a $\sim 15,000$ K star – although a double star or even a star cluster could not be ruled out. The spectrum is of relatively low resolution and not very deep but nevertheless a remarkable proof-of-concept: JWST can observe spectroscopically very distant stars. This added to the observed spectrum of another very intriguing lensed star candidate, *Godzilla*, at $z \sim 2.37$, which was measured both from the ground and with JWST (e.g. [208,209]), and a later JWST spectrum of Earendel [205].

Another game changer for lensed stars from JWST came with the observation of the first gravitational arc in Abell 370 - which has since earned the name 'the Dragon arc' given it resembles a fire-spitting dragon. Observations of the cluster revealed more than 40 caustic-crossing events in one pair of repeat observations (Fig. 13), superseding the total number of caustic-crossing events that had been detected to that date. Indeed, several programs continue with JWST to explore caustic crossing events and monitor the Dragon Arc as well, and the numbers of stars at cosmological distances should continue to be rapidly rising.

The fact that individual stars can be now seen to cosmological distances may at first glance be hard to fathom, given the extreme magnification needed. However, when doing the numbers, it becomes clear that not only can we detect such stars, but that in fact we are bound to detect them, and in abundance; a prediction JWST now realises.

3.6. Lensed supernovae and other exploding transients

Strongly lensed supernovae have been a long sought-after observation. Already 60 years ago it was proposed that strongly lensed supernovae could, through time delays, constrain the expansion rate of the Universe [211]. While the same idea has been now applied to lensed quasars [91,92], for decades, no multiply imaged supernova was found. The first multiply imaged supernova that was clearly detected, lensed by a cluster, was found in 2014 with *Hubble* behind the galaxy cluster MACS J1149.5+2223 [212]. The supernova exploded in a spiral arm of a multiply imaged galaxy at a redshift of $z \simeq 1.5$, further lensed by a local cluster galaxy into an Einstein cross. The supernova was named SN Refsdal, and spurred much excitement. Lens models predicted that another image of the supernova should appear about a year later in a different image of the spiral, a prediction that follow-up HST observations confirmed. SN Refsdal was then used to examine and improve lens models [71,213], and to put constraints on the

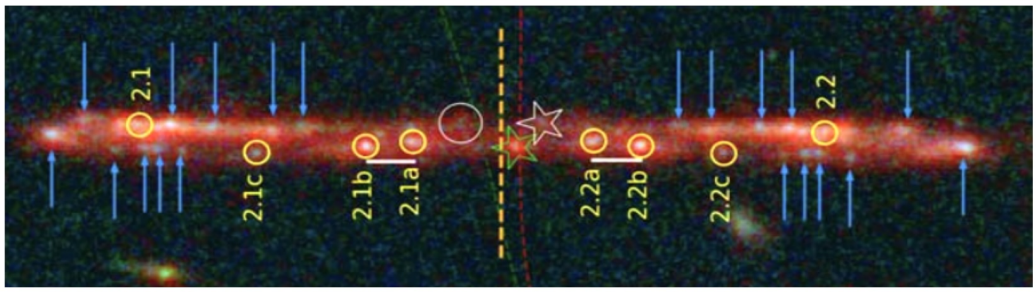


Figure 11. Lensed star candidates in an arc at $z \sim 4.8$, detected in JWST/NIRCam observations [199]. The figure shows two lensed star candidates (marked with a star shape) next to positions of the critical curves (dashed lines). The faint green and purple dashed lines show the critical curves from two different lens models, and the yellow dashed line marks the symmetry point of the arc. Counter images of various knots are marked with blue arrows, some of them also circled and numbered. Figure from [199].

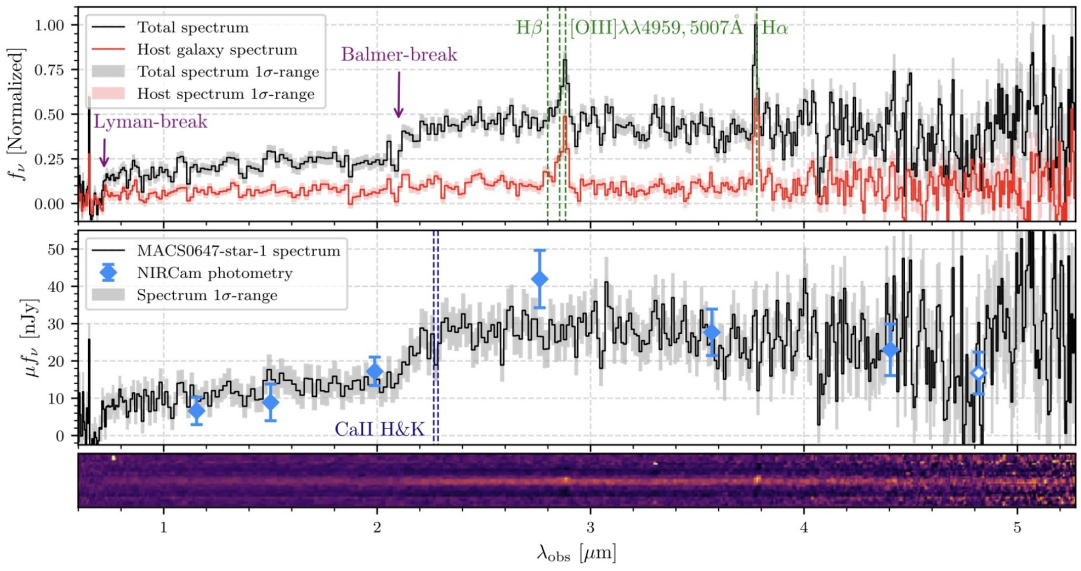


Figure 12. JWST can obtain spectra of stars at large cosmological distances. Figure shows the spectrum taken for the $z \simeq 4.8$ star marked in green in Fig. 11. The upper panel shows the total and the host's JWST/NIRSpec spectrum. The clean JWST/NIRSpec spectrum of the star is seen in the middle panel. The bottom panel shows the 2D spectrum of through the slit. The star's spectrum, while of relatively low resolution, constitutes a remarkable proof of concept of JWST capabilities: Only JWST coupled with lensing can perform a similar observation. The spectrum yielded a temperature of $\sim 15,000$ K for the star candidate in agreement with the photometric estimates, but a deeper, higher-resolution spectrum is needed to distinguish it from, e.g. a binary star system or a star cluster. Figure from [206].

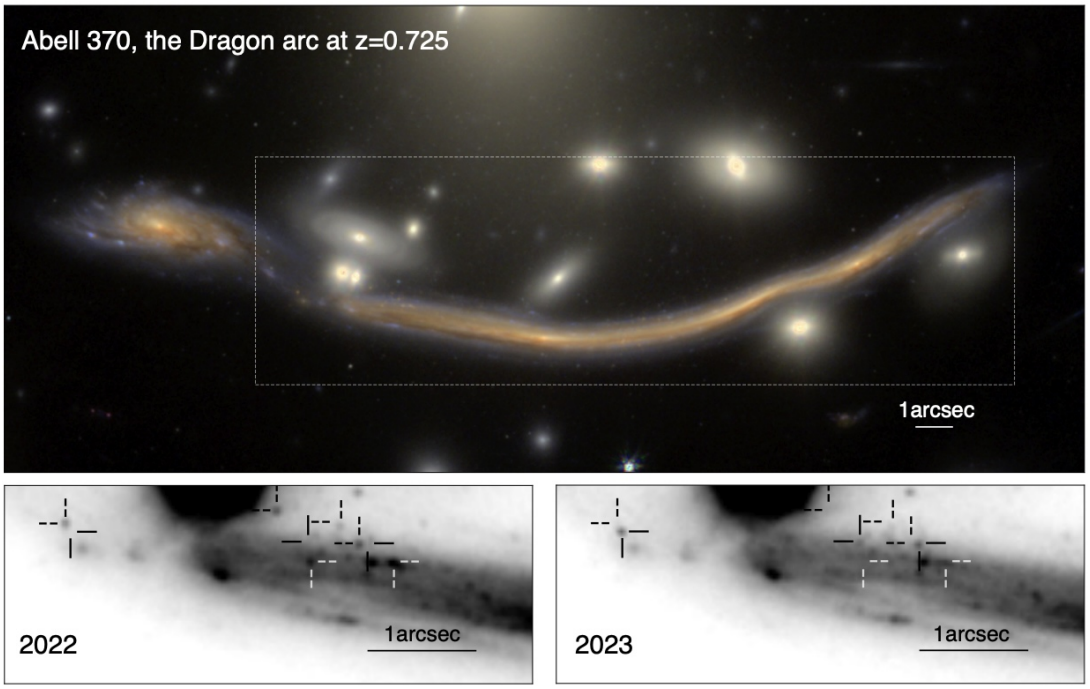


Figure 13. The first gravitational arc, seen in Abell 370 and now dubbed the Dragon, imaged with JWST. Imaging at two different epochs revealed over 40 transient point sources – stars in the background spiral galaxy sitting near the caustics and getting temporarily, highly magnified. The bottom panels show a portion of the arc at the two different epochs, and marked in (dashed) half-crosses are the locations of sources (dis-)appearing between the two epochs. Figure from [210].

expansion rate of the universe [214].

The fact that the lens models could predict where and when another image of the supernova would appear suggested that supernovae could thus be captured in their first moments of explosions. This is very important because the early light-curve evolution teaches us about the progenitor of the supernova and its environment [215,216]. Only a couple other multiply lensed supernovae have been detected with *Hubble* (e.g. [217]) and indeed, in at least one other instance, thanks to time delay, one of the images captured the supernova only hours after explosion, leading to constraints on the progenitor [218].

Lensed supernovae are also advantageous in other aspects. Lensing magnification allows us to see farther, and thus more distant supernovae could be observed through lensing. This should enable us to trace and understand stellar evolution through cosmic time, and potentially also observe rare explosions from massive, low-metallicity stars. Lensed supernovae of Type Ia could also then help in populating the Hubble diagram of brightness or distance versus redshift at the high redshift end, for stronger constraints on cosmology. Lensing of Type Ia supernovae, being standardisable candles, also supplies a precious test for the magnification estimates from different lens models [219,220].

JWST's increased resolution and depth turned out to be a key factor for detecting more multiply imaged supernovae. In just three years of operation JWST has detected more lensed SNe by galaxy clusters than *Hubble* [221–223], suggesting that many more are to come with ongoing and future surveys. The increased depth coupled with lensing magnification essentially opens up significantly more volume in which lensed

supernovae can be found per observation. While upcoming sky surveys from space such as Euclid and the Roman Space Telescope, or from the ground with large telescopes such as the Vera Rubin Observatory (LSST) are predicted to find many multiply imaged supernovae based on the much larger area probed and constant repeat visits, it was somewhat surprising – at least for those who got used to the detection rates from *Hubble* – that JWST essentially turned into a transient detection machine: The current rate implies that just a few visits to a massive, strong-lensing galaxy cluster with JWST are sufficient to yield a multiply imaged supernova.

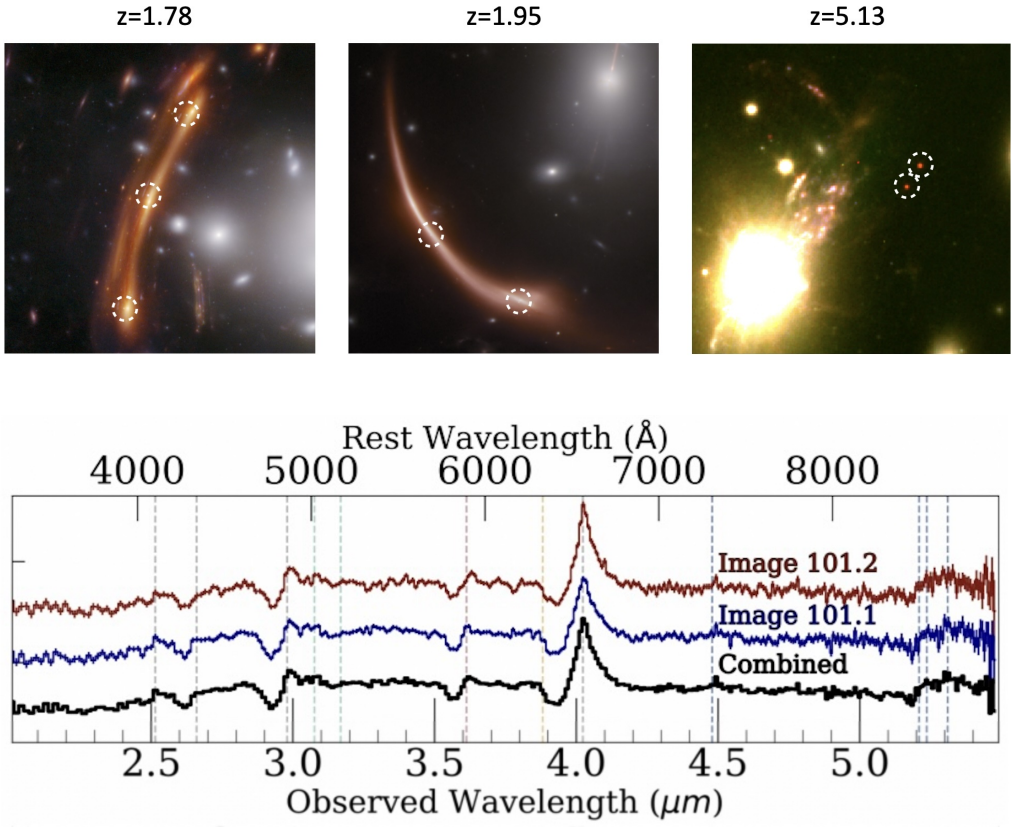


Figure 14. Multiply imaged supernovae detected with JWST. Upper row, Left: Supernova H0PE at $z = 1.78$ [222]. Middle: Supernova Encore at $z = 1.95$ [221]. Right: Supernova Eos – the farthest directly observed supernova to date, at $z = 5.13$ [224]. A spectrum of the supernova is seen in the lower panel, showing the relative flux density as a function of wavelength for the two supernova images, as well as their combined spectrum. The spectra were shifted vertically for better visibility. The spectra confirm that both images are counter-images of the same source – a metal-poor Type II supernova (subfigure adapted from [224], further cut and edited here). JWST is the only instrument capable of measuring the optical spectrum of this supernova, which was originally detected with JWST thanks to lensing [177].

JWST has recently observed the farthest, multiply imaged supernova at a redshift of $z = 5.13$, SN Eos ([224]; see Figure 14 here). While most supernovae are detected through difference imaging showing the appearance or disappearance of the SN compared to previous data, SN Eos was detected thanks to lensing: Two red point sources were noted in recent imaging of the galaxy cluster MACS J1931.8-2635. The position of the two red point-sources suggested they were likely counter images of the same background source, but the lack of counter images where the lens model predicted them suggested it was a transient source, a redshift $z \sim 5$ supernova [177]. Indeed, photometric and spectroscopic observations, and the absence of the SN images in pre-

vious *Hubble* data, confirmed this prediction [224], demonstrating the power of JWST in finding and studying distant and lensed supernovae.

It is worth mentioning that supernovae are not the only type of explosive transient sources that can be multiply imaged. The recent decade has seen increased interest in lensing of other transient sources such as Fast Radio Bursts, Gamma Ray Bursts, Tidal Disruption Events, or Gravitational Waves, and the range of science that can be done with them. While some of these cannot be directly observed with JWST, their progenitors or counterparts, could. It is thus safe to gamble that it is only a matter of time until more exciting supernovae or other transient results from JWST, will be delivered.

3.7. Galaxy-Cluster Evolution

Galaxy clusters are the most massive gravitationally bound structures in the Universe and are believed to form around $z \sim 3$. Clusters contain hundreds to thousands of galaxies, and as a result of interactions within the dense cluster which remove the gas from the constituent galaxies and thus the fuel for forming new stars, most of these galaxies are red ellipticals, brighter redwards of ∼4000-5000 Å rest-frame. JWST is thus an ideal observatory to investigate cluster evolution. The SLICE survey [225,226], for example, uses NIRCam to observe clusters out to nearly $z \sim 2$, tracking 8 Gyrs of formation history of massive clusters, chosen from Sunyaev-Zel'dovich and X-ray catalogues. The cluster mass-redshift evolution can address many aspects of cluster evolution, from the formation of Brightest Cluster Galaxies, through infalling cluster galaxies and the build-up of stellar, dark matter and intra-cluster light content, to the large population of globular clusters now visible with JWST [227–229].

Most lensing studies to date, due to a combination of cluster lensing efficiency and observational capabilities, have concentrated on clusters at redshifts around $\sim 0.2-0.5$, with some examples at somewhat higher redshifts towards $z \sim 1$. In recent years, however, clusters have also been detected to cosmic noon ($z \sim 2-3$), for example through their Sunyaev-Zel'dovich effect which does not experience redshift dimming, but their lensing signatures have been harder to capture. JWST now enables not only a deeper, longer-wavelength window into these clusters, but also into their magnified backgrounds, allowing us to derive reliable masses for them through strong (where apparent) and weak lensing. In fact, it turns out that JWST is an excellent instrument for weak-lensing studies [230–232]. While the field-of-view in JWST imaging is not very wide, its sensitivity and high spatial resolution reveal a high density of background sources and enable robust measurement of their ellipticities, and thus the shear signal.

In addition to massive clusters at cosmic noon, early overdensities, which are believed to be the seeds of these later-time massive clusters of galaxies, are visible with JWST to high redshifts. Indeed, such proto-clusters have been observed with JWST [233,234], including spectroscopically, with some lensed galaxy overdensities seen out to cosmic dawn where the Universe was less than a Gyr old [235–238]. The JWST, therefore, opens a precious window for studying the formation and evolution of clusters of galaxies through almost 14 Gyr of cosmic history!

4. Conclusion

One of the first images from JWST, released to the public in July 2022, was of a lensing cluster, SMACS J0723.3–7327, allowing a preview of JWST's capabilities. The

depth and amount of apparent detail, compared to previous images of the same cluster field, were astonishing: Stellar clumps and a variety of point sources in the cluster and in-and-around background galaxies were seen in great abundances, for the first time; high-redshift galaxies were observed and spectroscopically measured beyond the limit of our capabilities from the ground; high-redshift overdensities were discovered; and a variety of new lensed features have surfaced.

Over the next couple of years the exciting capabilities exhibited by the first JWST cluster image have continued to establish, deepen, and expand. Lensing campaigns in JWST's first few years of operations such as GLASS, UNCOVER, CANUCS, PEARLS, GLIMPSE, MAGNIF, SLICE, and VENUS, included both very deep observations of single clusters as well as shallower observations of growing samples of clusters, often with a component of follow-up spectroscopy or repeat observations for the study of potential transients. The number of clusters now covered with JWST in just a few cycles - by now many dozens of clusters have been observed – does not fall shy of that covered with *Hubble* in over 3 decades of operations. This is perhaps a testimony to the growing importance of lensing for studying dark matter, structure formation and cosmology and of course – the distant universe.

Although a large number of clusters has been covered with JWST, the rate at which new lensing related studies and discoveries emerge remains surprising. High-redshift galaxies are being detected to higher redshifts or fainter magnitudes beyond those that have been reachable with *Hubble*, often accompanied by UV and optical spectroscopy, and a detailed view of star-forming clumps, globular clusters, and galaxies such as spirals, can be seen to higher redshifts than ever before. Combined with lensing, JWST has opened new realms to study and discover – in particular, of small, point-like sources. Lensed SMBH and AGN are easier to spot with JWST and are seen to higher redshifts and smaller masses; star clusters that we could not resolve before are now seen within galaxy clusters at $z << 1$, around galaxies in cosmic noon, and down to 1 pc scales at highly magnified arcs at redshifts beyond $\sim 10 - 11$; redder and fainter sources previously elusive or completely unfamiliar have been detected, such as Little Red Dots; population III candidates have been found; and multiply imaged supernovae and extremely magnified lensed stars are being detected in greater numbers and towards higher redshifts than has been possible with *Hubble*.

The unique capabilities of JWST in terms of wavelength coverage, depth, and detail, also place it in excellent synergy with a range of instruments, such as the Atacama Large Millimeter/submillimeter Array (ALMA), Euclid mission, Vera Rubin observatory/LSST, the Nancy Grace Roman Space Telescope, and the upcoming 30-40m class of extremely large telescopes. For example, wide-field and survey instruments can scan the sky for intriguing objects and phenomena in the optical and infrared, with JWST then able to zoom-in on these objects and probe them in a unique range of wavelengths and to greater detail and depths. Further enhanced by the powers of gravitational lensing pushing JWST to see fainter and farther, we can anecdotally say: It is a bright future for faint sources.

Acknowledgement(s)

This work uses observations made with the NASA/ESA/CSA James Webb Space Telescope. The data were obtained from the Mikulski Archive for Space Telescopes (MAST) at the Space Telescope Science Institute (STScI), which is operated by the Association of Universities for Research in Astronomy (AURA), Inc., under NASA

contract NAS 5-03127 for JWST. Some of stamp images presented herein were constructed using reduced data retrieved from the Dawn JWST Archive (DJA; see also [239] for the `grizli` data-reduction software). DJA is an initiative of the Cosmic Dawn Center (DAWN), which is funded by the Danish National Research Foundation under grant DNRF140. Other stamp images include reduced data from the UNCOVER, PEARLS, or VENUS repositories, to which the author has internal access. I would like to kindly thank the respective teams and acknowledge the hard work put into obtaining and reducing these data and making them available. The author is also in debt to his research students, postdocs, and many collaborators, for many enriching discussions over the years. Finally, I would like to dedicate this review to Stella Seitz, Avishai Dekel, Mario Nonino, and Yannick Mellier; dear colleagues whom the lensing, high-redshift, and galaxy-evolution communities have lost over the past few years.

Funding

This work is supported by the Israel Science Foundation Grant No. 864/23.

References

[1] Ellis RS. Gravitational lensing: a unique probe of dark matter and dark energy. Philosophical Transactions of the Royal Society A: Mathematical, Physical and Engineering Sciences. 2010;368(1914):967–987.

[2] Meneghetti M. Introduction to gravitational lensing: With python examples. Springer International Publishing; 2021. Lecture Notes in Physics; Available from: `https://books.google.co.il/books?id=2HlMEAAAQBAJ`.

[3] Einstein A. Die Feldgleichungen der Gravitation. Sitzungsberichte der Königlich Preussischen Akademie der Wissenschaften. 1915 Jan;:844–847.

[4] Einstein A. Die Grundlage der allgemeinen Relativitätstheorie. Annalen der Physik. 1916 Jan;354(7):769–822.

[5] Dyson FW, Eddington AS, Davidson C. A Determination of the Deflection of Light by the Sun's Gravitational Field, from Observations Made at the Total Eclipse of May 29, 1919. Philosophical Transactions of the Royal Society of London Series A. 1920 Jan; 220:291–333.

[6] Walsh D, Carswell RF, Weymann RJ. 0957+561 A, B: twin quasistellar objects or gravitational lens? Nature. 1979 May;279:381–384.

[7] Huchra J, Gorenstein M, Kent S, et al. 2237+0305 : a new and unusual gravitational lens. Astron. J.. 1985 May;90:691–696.

[8] Lynds R, Petrosian V. Giant Luminous Arcs in Galaxy Clusters. In: Bulletin of the American Astronomical Society; Vol. 18; Sep.; 1986. p. 1014.

[9] Soucail G, Fort B, Mellier Y, et al. A blue ring-like structure, in the center of the A 370 cluster of galaxies. Astron. Astrophys.. 1987 Jan;172:L14–L16.

[10] Lynds R, Petrosian V. Luminous Arcs in Clusters of Galaxies. Astrophys. J.. 1989 Jan; 336:1.

[11] Soucail G, Mellier Y, Fort B, et al. The giant arc in A 370 : spectroscopic evidence for gravitational lensing from a source at Z=0.724. Astron. Astrophys.. 1988 Feb;191:L19–L21.

[12] Paczynski B. Giant luminous arcs discovered in two clusters of galaxies. Nature. 1987 Feb;325(6105):572–573.

[13] Tyson JA, Valdes F, Wenk RA. Detection of Systematic Gravitational Lens Galaxy

Image Alignments: Mapping Dark Matter in Galaxy Clusters. Astrophys. J. Lett.. 1990 Jan;349:L1.
[14] Kaiser N, Squires G. Mapping the Dark Matter with Weak Gravitational Lensing. Astrophys. J.. 1993 Feb;404:441.
[15] Kaiser N, Squires G, Broadhurst T. A Method for Weak Lensing Observations. Astrophys. J.. 1995 Aug;449:460.
[16] Kneib JP, Mellier Y, Fort B, et al. The Distribution of Dark Matter in Distant Cluster Lenses - Modelling A:370. Astron. Astrophys.. 1993 Jun;273:367.
[17] Kneib JP, Ellis RS, Smail I, et al. Hubble Space Telescope Observations of the Lensing Cluster Abell 2218. Astrophys. J.. 1996 Nov;471:643.
[18] Kneib JP, Ellis RS, Santos MR, et al. A Probable z˜7 Galaxy Strongly Lensed by the Rich Cluster A2218: Exploring the Dark Ages. Astrophys. J.. 2004 Jun;607:697–703.
[19] Smith GP, Kneib JP, Smail I, et al. A Hubble Space Telescope lensing survey of X-ray luminous galaxy clusters - IV. Mass, structure and thermodynamics of cluster cores at z= 0.2. Mon. Not. R. Astron. Soc.. 2005 May;359(2):417–446.
[20] Broadhurst T, Benítez N, Coe D, et al. Strong-Lensing Analysis of A1689 from Deep Advanced Camera Images. Astrophys. J.. 2005 Mar;621:53–88.
[21] Broadhurst T, Takada M, Umetsu K, et al. The Surprisingly Steep Mass Profile of A1689, from a Lensing Analysis of Subaru Images. Astrophys. J. Lett.. 2005 Feb;619:L143–L146.
[22] Halkola A, Seitz S, Pannella M. Parametric strong gravitational lensing analysis of Abell 1689. Mon. Not. R. Astron. Soc.. 2006 Nov;372:1425–1462.
[23] Jullo E, Kneib JP. Multiscale cluster lens mass mapping - I. Strong lensing modelling. Mon. Not. R. Astron. Soc.. 2009 May;395:1319–1332.
[24] Liesenborgs J, De Rijcke S, Dejonghe H. A genetic algorithm for the non-parametric inversion of strong lensing systems. Mon. Not. R. Astron. Soc.. 2006 Apr;367:1209–1216.
[25] Zitrin A, Broadhurst T, Umetsu K, et al. New multiply-lensed galaxies identified in ACS/NIC3 observations of Cl0024+1654 using an improved mass model. Mon. Not. R. Astron. Soc.. 2009 Jul;396:1985–2002.
[26] Ebeling H, Edge AC, Henry JP. MACS: A Quest for the Most Massive Galaxy Clusters in the Universe. Astrophys. J.. 2001 Jun;553:668–676.
[27] Richard J, Smith GP, Kneib JP, et al. LoCuSS: first results from strong-lensing analysis of 20 massive galaxy clusters at z = 0.2. Mon. Not. R. Astron. Soc.. 2010 May;404:325–349.
[28] Postman M, Coe D, Benítez N, et al. The Cluster Lensing and Supernova Survey with Hubble: An Overview. Astrophys. J. Suppl. Ser.. 2012 Apr;199:25.
[29] Coe D, Salmon B, Bradač M, et al. RELICS: Reionization Lensing Cluster Survey. Astrophys. J.. 2019 Oct;884(1):85.
[30] Zheng W, Postman M, Zitrin A, et al. A magnified young galaxy from about 500 million years after the Big Bang. Nature. 2012 Sep;489:406–408.
[31] Coe D, Zitrin A, Carrasco M, et al. CLASH: Three Strongly Lensed Images of a Candidate z ≈ 11 Galaxy. Astrophys. J.. 2013 Jan;762(1):32.
[32] Lotz JM, Koekemoer A, Coe D, et al. The Frontier Fields: Survey Design and Initial Results. Astrophys. J.. 2017 Mar;837:97.
[33] Oguri M, Bayliss MB, Dahle H, et al. Combined strong and weak lensing analysis of 28 clusters from the Sloan Giant Arcs Survey. Mon. Not. R. Astron. Soc.. 2012 Mar; 420(4):3213–3239.
[34] Merten J, Meneghetti M, Postman M, et al. CLASH: The Concentration-Mass Relation of Galaxy Clusters. Astrophys. J.. 2015 Jun;806(1):4.
[35] Umetsu K, Medezinski E, Nonino M, et al. CLASH: Weak-lensing Shear-and-magnification Analysis of 20 Galaxy Clusters. Astrophys. J.. 2014 Nov;795:163.
[36] Umetsu K. Cluster-galaxy weak lensing. Astron. Astrophys. Rev.. 2020 Dec;28(1):7.
[37] Stern C, Dietrich JP, Bocquet S, et al. Weak-lensing analysis of SPT-selected galaxy clusters using Dark Energy Survey Science Verification data. Mon. Not. R. Astron. Soc.. 2019 May;485(1):69–87.

[38] Sereno M, Covone G, Izzo L, et al. PSZ2LenS. Weak lensing analysis of the Planck clusters in the CFHTLenS and in the RCSLenS. Mon. Not. R. Astron. Soc.. 2017 Dec; 472(2):1946–1971.
[39] Hoekstra H, Herbonnet R, Muzzin A, et al. The Canadian Cluster Comparison Project: detailed study of systematics and updated weak lensing masses. Mon. Not. R. Astron. Soc.. 2015 May;449(1):685–714.
[40] Gruen D, Seitz S, Brimioulle F, et al. Weak lensing analysis of SZ-selected clusters of galaxies from the SPT and Planck surveys. Mon. Not. R. Astron. Soc.. 2014 Aug; 442(2):1507–1544.
[41] Udalski A, Szymanski M, Kaluzny J, et al. The Optical Gravitational Lensing Experiment. Acta Astron.. 1992 Oct;42:253–284.
[42] Sumi T, Abe F, Bond IA, et al. Microlensing Optical Depth toward the Galactic Bulge from Microlensing Observations in Astrophysics Group Observations during 2000 with Difference Image Analysis. Astrophys. J.. 2003 Jul;591(1):204–227.
[43] Tisserand P, Le Guillou L, Afonso C, et al. Limits on the Macho content of the Galactic Halo from the EROS-2 Survey of the Magellanic Clouds. Astron. Astrophys.. 2007 Jul; 469(2):387–404.
[44] Treu T. Strong Lensing by Galaxies. Annu. Rev. Astron. Astrophys.. 2010 Sep;48:87–125.
[45] Surdej J. Observational aspects of gravitational lensing. In: Mellier Y, Fort B, Soucail G, editors. Gravitational lensing. Vol. 360; 1990. p. 57–72.
[46] Surdej J, Refsdal S, Pospieszalska-Surdej A. The optical gravitational lens experiment. In: Surdej J, Fraipont-Caro D, Gosset E, et al., editors. Liege International Astrophysical Colloquia; (Liege International Astrophysical Colloquia; Vol. 31); Jan.; 1993. p. 199.
[47] Schneider P. A new formulation of gravitational lens theory, time-delay, and Fermat's principle. Astron. Astrophys.. 1985 Feb;143:413–420.
[48] Blandford R, Narayan R. Fermat's principle, caustics, and the classification of gravitational lens images. Astrophys. J.. 1986 Nov;310:568–582.
[49] Narayan R, Bartelmann M. Lectures on Gravitational Lensing. ArXiv Astrophysics e-prints. 1996 Jun;astro-ph/9606001.
[50] Berry M. Waves and thom's theorem. Advances in Physics. 1976;25(1):1–26. Available from: https://doi.org/10.1080/00018737600101342.
[51] Schneider P, Ehlers J, Falco EE. Gravitational Lenses. ; 1992.
[52] Kneib JP, Natarajan P. Cluster lenses. Astron. Astrophys. Rev.. 2011 Nov;19:47.
[53] Meylan G, Jetzer P, North P, et al., editors. Gravitational Lensing: Strong, Weak and Micro; 2006.
[54] Merritt D, Graham AW, Moore B, et al. Empirical Models for Dark Matter Halos. I. Nonparametric Construction of Density Profiles and Comparison with Parametric Models. Astron. J.. 2006 Dec;132(6):2685–2700.
[55] Niemiec A, Jauzac M, Eckert D, et al. Beyond the ultradeep frontier fields and legacy observations (BUFFALO): a high-resolution strong+weak-lensing view of Abell 370. Mon. Not. R. Astron. Soc.. 2023 Sep;524(2):2883–2910.
[56] Fischer P, McKay TA, Sheldon E, et al. Weak Lensing with Sloan Digital Sky Survey Commissioning Data: The Galaxy-Mass Correlation Function to 1 H^{-1} Mpc. Astron. J.. 2000 Sep;120(3):1198–1208.
[57] Euclid Collaboration, Mellier Y, Abdurro'uf, et al. Euclid: I. Overview of the Euclid mission. Astron. Astrophys.. 2025 May;697:A1.
[58] Ivezić Ž, Kahn SM, Tyson JA, et al. LSST: From Science Drivers to Reference Design and Anticipated Data Products. Astrophys. J.. 2019 Mar;873(2):111.
[59] Mao S, Paczynski B. Gravitational Microlensing by Double Stars and Planetary Systems. Astrophys. J. Lett.. 1991 Jun;374:L37.
[60] Gould A, Loeb A. Discovering Planetary Systems through Gravitational Microlenses. Astrophys. J.. 1992 Sep;396:104.
[61] Atek H, Chisholm J, Kokorev V, et al. JWST's GLIMPSE: an overview of the deepest probe of early galaxy formation and cosmic reionization. arXiv e-prints. 2025 Nov;

:arXiv:2511.07542.
[62] Zitrin A, Broadhurst T, Rephaeli Y, et al. The Largest Gravitational Lens: MACS J0717.5+3745 (z = 0.546). Astrophys. J. Lett.. 2009 Dec;707:L102–L106.
[63] Diego JM, Protopapas P, Sandvik HB, et al. Non-parametric inversion of strong lensing systems. Mon. Not. R. Astron. Soc.. 2005 Jun;360:477–491.
[64] Williams LLR, Saha P. Pixelated Lenses and H_0 from Time-Delay Quasars. Astron. J.. 2000 Feb;119(2):439–450.
[65] Wagner J, Liesenborgs J, Tessore N. Model-independent and model-based local lensing properties of CL0024+1654 from multiply imaged galaxies. Astron. Astrophys.. 2018 Apr;612:A17.
[66] Jullo E, Kneib JP, Limousin M, et al. A Bayesian approach to strong lensing modelling of galaxy clusters. New Journal of Physics. 2007 Dec;9:447.
[67] Oguri M, Takada M, Okabe N, et al. Direct measurement of dark matter halo ellipticity from two-dimensional lensing shear maps of 25 massive clusters. Mon. Not. R. Astron. Soc.. 2010 Jul;405:2215–2230.
[68] Suyu SH, Acebron A, Grillo C, et al. Cosmology with supernova Encore in the strong lensing cluster MACS J0138-2155: Lens model comparison and H_0 measurement. Astron. Astrophys.. 2026 Apr;708:A291.
[69] Host O. Galaxy cluster strong lensing: image deflections from density fluctuations along the line of sight. Mon. Not. R. Astron. Soc.. 2012 Feb;420:L18–L22.
[70] Bergamini P, Rosati P, Mercurio A, et al. Enhanced cluster lensing models with measured galaxy kinematics. Astron. Astrophys.. 2019 Nov;631:A130.
[71] Treu T, Brammer G, Diego JM, et al. "Refsdal" Meets Popper: Comparing Predictions of the Re-appearance of the Multiply Imaged Supernova Behind MACSJ1149.5+2223. Astrophys. J.. 2016 Jan;817:60.
[72] Meneghetti M, Natarajan P, Coe D, et al. The Frontier Fields lens modelling comparison project. Mon. Not. R. Astron. Soc.. 2017 Dec;472(3):3177–3216.
[73] Franx M, Illingworth GD, Kelson DD, et al. A Pair of Lensed Galaxies at z=4.92 in the Field of CL 1358+62. Astrophys. J. Lett.. 1997 Sep;486:L75.
[74] Richard J, Kneib JP, Ebeling H, et al. Discovery of a possibly old galaxy at z= 6.027, multiply imaged by the massive cluster Abell 383. Mon. Not. R. Astron. Soc.. 2011 Jun; 414(1):L31–L35.
[75] Monna A, Seitz S, Greisel N, et al. CLASH: z $\sim$ 6 young galaxy candidate quintuply lensed by the frontier field cluster RXC J2248.7-4431. Mon. Not. R. Astron. Soc.. 2014 Feb;438:1417–1434.
[76] Zitrin A, Zheng W, Broadhurst T, et al. A Geometrically Supported z ˜ 10 Candidate Multiply Imaged by the Hubble Frontier Fields Cluster A2744. Astrophys. J. Lett.. 2014 Sep;793:L12.
[77] Bradley LD, Bouwens RJ, Ford HC, et al. Discovery of a Very Bright Strongly Lensed Galaxy Candidate at z ˜ 7.6. Astrophys. J.. 2008 May;678:647–654.
[78] Ellis RS, McLure RJ, Dunlop JS, et al. The Abundance of Star-forming Galaxies in the Redshift Range 8.5-12: New Results from the 2012 Hubble Ultra Deep Field Campaign. Astrophys. J. Lett.. 2013 Jan;763:L7.
[79] Bouwens RJ, Illingworth GD, Oesch PA, et al. UV Luminosity Functions at Redshifts z $\sim$ 4 to z $\sim$ 10: 10,000 Galaxies from HST Legacy Fields. Astrophys. J.. 2015 Apr;803:34.
[80] Oesch PA, Brammer G, van Dokkum PG, et al. A Remarkably Luminous Galaxy at z=11.1 Measured with Hubble Space Telescope Grism Spectroscopy. Astrophys. J.. 2016 Mar;819:129.
[81] Finkelstein SL, Ryan RE Jr, Papovich C, et al. The Evolution of the Galaxy Rest-frame Ultraviolet Luminosity Function over the First Two Billion Years. Astrophys. J.. 2015 Sep;810:71.
[82] Broadhurst TJ, Taylor AN, Peacock JA. Mapping cluster mass distributions via gravitational lensing of background galaxies. Astrophys. J.. 1995 Jan;438:49–61.
[83] Atek H, Richard J, Kneib JP, et al. The extreme faint end of the UV luminosity function

at z $z \sim 6$ through gravitational telescopes: a comprehensive assessment of strong lensing uncertainties. Mon. Not. R. Astron. Soc.. 2018 Oct;479(4):5184–5195.

[84] Ishigaki M, Kawamata R, Ouchi M, et al. Hubble Frontier Fields First Complete Cluster Data: Faint Galaxies at z ˜ 5-10 for UV Luminosity Functions and Cosmic Reionization. Astrophys. J.. 2015 Jan;799:12.

[85] Clowe D, Bradač M, Gonzalez AH, et al. A Direct Empirical Proof of the Existence of Dark Matter. Astrophys. J. Lett.. 2006 Sep;648:L109–L113.

[86] Bradač M, Clowe D, Gonzalez AH, et al. Strong and Weak Lensing United. III. Measuring the Mass Distribution of the Merging Galaxy Cluster 1ES 0657-558. Astrophys. J.. 2006 Dec;652:937–947.

[87] Markevitch M, Gonzalez AH, Clowe D, et al. Direct Constraints on the Dark Matter Self-Interaction Cross Section from the Merging Galaxy Cluster 1E 0657-56. Astrophys. J.. 2004 May;606(2):819–824.

[88] Voit GM. Tracing cosmic evolution with clusters of galaxies. Reviews of Modern Physics. 2005 Apr;77(1):207–258.

[89] Siegel SR, Sayers J, Mahdavi A, et al. Constraints on the Mass, Concentration, and Nonthermal Pressure Support of Six CLASH Clusters from a Joint Analysis of X-Ray, SZ, and Lensing Data. Astrophys. J.. 2018 Jul;861(1):71.

[90] Sereno M, Umetsu K, Ettori S, et al. CLUMP-3D: Testing ΛCDM with Galaxy Cluster Shapes. Astrophys. J. Lett.. 2018 Jun;860(1):L4.

[91] Suyu SH, Bonvin V, Courbin F, et al. H0LiCOW - I. H_0 Lenses in COSMOGRAIL's Wellspring: program overview. Mon. Not. R. Astron. Soc.. 2017 Jul;468(3):2590–2604.

[92] Wong KC, Suyu SH, Chen GCF, et al. H0LiCOW - XIII. A 2.4 per cent measurement of H_0 from lensed quasars: 5.3σ tension between early- and late-Universe probes. Mon. Not. R. Astron. Soc.. 2020 Oct;498(1):1420–1439.

[93] Riess AG, Casertano S, Yuan W, et al. Cosmic Distances Calibrated to 1% Precision with Gaia EDR3 Parallaxes and Hubble Space Telescope Photometry of 75 Milky Way Cepheids Confirm Tension with ΛCDM. Astrophys. J. Lett.. 2021 Feb;908(1):L6.

[94] Freedman WL. Measurements of the Hubble Constant: Tensions in Perspective. Astrophys. J.. 2021 Sep;919(1):16.

[95] Planck Collaboration, Aghanim N, Akrami Y, et al. Planck 2018 results. VI. Cosmological parameters. Astron. Astrophys.. 2020 Sep;641:A6.

[96] Jullo E, Natarajan P, Kneib J, et al. Cosmological Constraints from Strong Gravitational Lensing in Clusters of Galaxies. Science. 2010 Aug;329:924–927.

[97] Chemerynska I, Atek H, Furtak LJ, et al. The first GLIMPSE of the faint galaxy population at Cosmic Dawn with JWST: The evolution of the ultraviolet luminosity function across z $\sim 9-15$. Mon. Not. R. Astron. Soc.. 2026 Feb;546(2):staf2267.

[98] Adams NJ, Conselice CJ, Ferreira L, et al. Discovery and properties of ultra-high redshift galaxies (9 ¡ z ¡ 12) in the JWST ERO SMACS 0723 Field. Mon. Not. R. Astron. Soc.. 2023 Jan;518(3):4755–4766.

[99] Donnan CT, McLure RJ, Dunlop JS, et al. JWST PRIMER: a new multifield determination of the evolving galaxy UV luminosity function at redshifts z $\simeq$ 9 - 15. Mon. Not. R. Astron. Soc.. 2024 Sep;533(3):3222–3237.

[100] Leung GCK, Bagley MB, Finkelstein SL, et al. NGDEEP Epoch 1: The Faint End of the Luminosity Function at z 9-12 from Ultradeep JWST Imaging. Astrophys. J. Lett.. 2023 Sep;954(2):L46.

[101] Finkelstein SL, Leung GCK, Bagley MB, et al. The Complete CEERS Early Universe Galaxy Sample: A Surprisingly Slow Evolution of the Space Density of Bright Galaxies at z $\sim$ 8.5–14.5. Astrophys. J. Lett.. 2024 Jul;969(1):L2.

[102] Kokorev V, Atek H, Chisholm J, et al. A Glimpse of the New Redshift Frontier through AS1063. Astrophys. J. Lett.. 2025 Apr;983(1):L22.

[103] Harikane Y, Nakajima K, Ouchi M, et al. Pure Spectroscopic Constraints on UV Luminosity Functions and Cosmic Star Formation History from 25 Galaxies at z $_{spec}$ = 8.61-13.20 Confirmed with JWST/NIRSpec. Astrophys. J.. 2024 Jan;960(1):56.

[104] Bowler RAA, Jarvis MJ, Dunlop JS, et al. A lack of evolution in the very bright end of the galaxy luminosity function from z $\simeq$ 8 to 10. Mon. Not. R. Astron. Soc.. 2020 Apr; 493(2):2059–2084.
[105] Wyder TK, Treyer MA, Milliard B, et al. The Ultraviolet Galaxy Luminosity Function in the Local Universe from GALEX Data. Astrophys. J. Lett.. 2005 Jan;619(1):L15–L18.
[106] Moutard T, Sawicki M, Arnouts S, et al. UV and U-band luminosity functions from CLAUDS and HSC-SSP - I. Using four million galaxies to simultaneously constrain the very faint and bright regimes to z $\sim$ 3. Mon. Not. R. Astron. Soc.. 2020 May;494(2):1894–1918.
[107] Bouwens RJ, Illingworth G, Ellis RS, et al. z 2-9 Galaxies Magnified by the Hubble Frontier Field Clusters. II. Luminosity Functions and Constraints on a Faint-end Turnover. Astrophys. J.. 2022 Nov;940(1):55.
[108] Schechter P. An analytic expression for the luminosity function for galaxies. Astrophys. J.. 1976 Jan;203:297–306.
[109] Ishigaki M, Kawamata R, Ouchi M, et al. Full-data Results of Hubble Frontier Fields: UV Luminosity Functions at z $\sim$ 6-10 and a Consistent Picture of Cosmic Reionization. Astrophys. J.. 2018 Feb;854:73.
[110] Livermore RC, Finkelstein SL, Lotz JM. Directly Observing the Galaxies Likely Responsible for Reionization. Astrophys. J.. 2017 Feb;835(2):113.
[111] Bouwens RJ, Oesch PA, Illingworth GD, et al. The z $\sim$ 6 Luminosity Function Fainter than -15 mag from the Hubble Frontier Fields: The Impact of Magnification Uncertainties. Astrophys. J.. 2017 Jul;843(2):129.
[112] Treu T, Roberts-Borsani G, Bradac M, et al. The GLASS-JWST Early Release Science Program. I. Survey Design and Release Plans. Astrophys. J.. 2022 Aug;935(2):110.
[113] Willott CJ, Doyon R, Albert L, et al. The Near-infrared Imager and Slitless Spectrograph for the James Webb Space Telescope. II. Wide Field Slitless Spectroscopy. Publ. Astron. Soc. Pac.. 2022 Feb;134(1032):025002.
[114] Sarrouh GTE, Asada Y, Martis NS, et al. CANUCS/Technicolor Data Release 1: Imaging, Photometry, Slit Spectroscopy, and Stellar Population Parameters. Astrophys. J. Suppl. Ser.. 2026 Jan;282(1):3.
[115] Windhorst RA, Cohen SH, Jansen RA, et al. JWST PEARLS. Prime Extragalactic Areas for Reionization and Lensing Science: Project Overview and First Results. Astron. J.. 2023 Jan;165(1):13.
[116] Bezanson R, Labbe I, Whitaker KE, et al. The JWST UNCOVER Treasury Survey: Ultradeep NIRSpec and NIRCam Observations before the Epoch of Reionization. Astrophys. J.. 2024 Oct;974(1):92.
[117] Atek H, Labbé I, Furtak LJ, et al. Most of the photons that reionized the Universe came from dwarf galaxies. Nature. 2024 Feb;626(8001):975–978.
[118] Fujimoto S, Naidu RP, Chisholm J, et al. GLIMPSE: An Ultrafaint $\simeq 10^5$ $M_\odot$ Pop III Galaxy Candidate and First Constraints on the Pop III UV Luminosity Function at z $\simeq$ 6–7. Astrophys. J.. 2025 Aug;989(1):46.
[119] Nakane M, Kokorev V, Fujimoto S, et al. VENUS: A Strongly Lensed Clumpy Galaxy at $z \sim 11 - 12$ behind the Galaxy Cluster MACS J0257.1-2325. arXiv e-prints. 2025 Nov;:arXiv:2511.14483.
[120] Curtis-Lake E, Carniani S, Cameron A, et al. Spectroscopic confirmation of four metal-poor galaxies at z = 10.3-13.2. Nature Astronomy. 2023 May;7:622–632.
[121] Carniani S, Hainline K, D'Eugenio F, et al. Spectroscopic confirmation of two luminous galaxies at a redshift of 14. Nature. 2024 Sep;633(8029):318–322.
[122] Naidu RP, Oesch PA, Brammer G, et al. A Cosmic Miracle: A Remarkably Luminous Galaxy at zspec = 14.44 Confirmed with JWST. The Open Journal of Astrophysics. 2026 Jan;9:56033.
[123] Hainline KN, Eisenstein DJ, Whitler L, et al. JWST Advanced Deep Extragalactic Survey (JADES) Data Release 5: Photometrically Selected Galaxy Candidates at z ¿ 8. arXiv e-prints. 2026 Jan;:arXiv:2601.15959.

[124] Wang B, Fujimoto S, Labbé I, et al. UNCOVER: Illuminating the Early Universe-JWST/NIRSpec Confirmation of z ¿ 12 Galaxies. Astrophys. J. Lett.. 2023 Nov; 957(2):L34.
[125] Castellano M, Napolitano L, Fontana A, et al. JWST NIRSpec Spectroscopy of the Remarkable Bright Galaxy GHZ2/GLASS-z12 at Redshift 12.34. Astrophys. J.. 2024 Sep;972(2):143.
[126] Roberts-Borsani G, Treu T, Shapley A, et al. Between the Extremes: A JWST Spectroscopic Benchmark for High-redshift Galaxies Using ∼500 Confirmed Sources at z ≥ 5. Astrophys. J.. 2024 Dec;976(2):193.
[127] Salmon B, Coe D, Bradley L, et al. RELICS: The Reionization Lensing Cluster Survey and the Brightest High-z Galaxies. Astrophys. J.. 2020 Feb;889(2):189.
[128] Bouwens RJ, Illingworth GD, Labbe I, et al. A candidate redshift z˜10 galaxy and rapid changes in that population at an age of 500Myr. Nature. 2011 Jan;469:504–507.
[129] Robertson BE, Tacchella S, Johnson BD, et al. Identification and properties of intense star-forming galaxies at redshifts z ¿ 10. Nature Astronomy. 2023 May;7:611–621.
[130] Harikane Y, Inoue AK, Ellis RS, et al. JWST, ALMA, and Keck Spectroscopic Constraints on the UV Luminosity Functions at z ∼ 7-14: Clumpiness and Compactness of the Brightest Galaxies in the Early Universe. Astrophys. J.. 2025 Feb;980(1):138.
[131] Napier K, Sharon K, Dahle H, et al. Hubble Constant Measurement from Three Large-separation Quasars Strongly Lensed by Galaxy Clusters. Astrophys. J.. 2023 Dec; 959(2):134.
[132] Hezaveh YD, Dalal N, Marrone DP, et al. Detection of Lensing Substructure Using ALMA Observations of the Dusty Galaxy SDP.81. Astrophys. J.. 2016 May;823(1):37.
[133] Mediavilla E, Muñoz JA, Kochanek CS, et al. The Structure of the Accretion Disk in the Lensed Quasar SBS 0909+532. Astrophys. J.. 2011 Mar;730(1):16.
[134] Williams PR, Treu T, Dahle H, et al. The Black Hole Mass of the z = 2.805 Multiply Imaged Quasar SDSS J2222+2745 from Velocity-resolved Time Lags of the C IV Emission Line. Astrophys. J.. 2021 Apr;911(1):64.
[135] Golubchik M, Steinhardt CL, Zitrin A, et al. Reverberation Mapping of High-mass and High-redshift Quasars Using Gravitational Time Delays. Astrophys. J.. 2024 Nov; 976(1):108.
[136] Inada N, Oguri M, Pindor B, et al. A gravitationally lensed quasar with quadruple images separated by 14.62arcseconds. Nature. 2003 Dec;426(6968):810–812.
[137] Inada N, Oguri M, Morokuma T, et al. SDSS J1029+2623: A Gravitationally Lensed Quasar with an Image Separation of 22.5". Astrophys. J. Lett.. 2006 Dec;653(2):L97–L100.
[138] Dahle H, Gladders MD, Sharon K, et al. SDSS J2222+2745: A Gravitationally Lensed Sextuple Quasar with a Maximum Image Separation of 15."1 Discovered in the Sloan Giant Arcs Survey. Astrophys. J.. 2013 Aug;773(2):146.
[139] Oguri M, Schrabback T, Jullo E, et al. The Hidden Fortress: structure and substructure of the complex strong lensing cluster SDSS J1029+2623. Mon. Not. R. Astron. Soc.. 2013 Feb;429(1):482–493.
[140] Sharon K, Bayliss MB, Dahle H, et al. Lens Model and Time Delay Predictions for the Sextuply Lensed Quasar SDSS J2222+2745. Astrophys. J.. 2017 Jan;835(1):5.
[141] Shu Y, Marques-Chaves R, Evans NW, et al. SDSS J0909+4449: A large-separation strongly lensed quasar at z ∼ 2.8 with three images. Mon. Not. R. Astron. Soc.. 2018 Nov;481(1):L136–L140.
[142] Bogdán Á, Kovács OE, Jones C, et al. Exploring Gravitationally Lensed z ≳ 6 X-Ray Active Galactic Nuclei Behind the RELICS Clusters. Astrophys. J.. 2022 Mar;927(1):34.
[143] Martinez MN, Napier KA, Cloonan AP, et al. COOL-LAMPS. III. Discovery of a 25."9 Separation Quasar Lensed by a Merging Galaxy Cluster. Astrophys. J.. 2023 Apr; 946(2):63.
[144] Ducourant C, Teixeira R, Vale-Cunha PH, et al. Gaia GraL: The GraL catalogue of gravitationally lensed quasars: X. Matched with Gaia data, redshifts, and time delays.

Astron. Astrophys.. 2026 Mar;707:A345.
[145] Furtak LJ, Mainali R, Zitrin A, et al. A variable active galactic nucleus at z = 2.06 triply-imaged by the galaxy cluster MACS J0035.4-2015. Mon. Not. R. Astron. Soc.. 2023 Jul;522(4):5142–5151.
[146] Furtak LJ, Zitrin A, Plat A, et al. JWST UNCOVER: Extremely Red and Compact Object at z $_{phot}$ $\simeq$ 7.6 Triply Imaged by A2744. Astrophys. J.. 2023 Aug;952(2):142.
[147] Allingham JFV, Zitrin A, Golubchik M, et al. SLICE: SPT-CL J0546-5345—A Prominent Strong-lensing Cluster at z = 1.07. Astrophys. J. Lett.. 2025 Sep;990(1):L25.
[148] Harikane Y, Zhang Y, Nakajima K, et al. A JWST/NIRSpec First Census of Broad-line AGNs at z = 4-7: Detection of 10 Faint AGNs with M $_{BH}$ 10^6-10^8 M $_\odot$ and Their Host Galaxy Properties. Astrophys. J.. 2023 Dec;959(1):39.
[149] Kocevski DD, Onoue M, Inayoshi K, et al. Hidden Little Monsters: Spectroscopic Identification of Low-mass, Broad-line AGNs at z ¿ 5 with CEERS. Astrophys. J. Lett.. 2023 Sep;954(1):L4.
[150] Atek H, Richard J, Kneib JP, et al. Probing the z ¿ 6 Universe with the First Hubble Frontier Fields Cluster A2744. Astrophys. J.. 2014 May;786:60.
[151] Labbé I, van Dokkum P, Nelson E, et al. A population of red candidate massive galaxies 600 Myr after the Big Bang. Nature. 2023 Apr;616(7956):266–269.
[152] Furtak LJ, Labbé I, Zitrin A, et al. A high black-hole-to-host mass ratio in a lensed AGN in the early Universe. Nature. 2024 Apr;628(8006):57–61.
[153] Matthee J, Naidu RP, Brammer G, et al. Little Red Dots: An Abundant Population of Faint Active Galactic Nuclei at z $\sim$ 5 Revealed by the EIGER and FRESCO JWST Surveys. Astrophys. J.. 2024 Mar;963(2):129.
[154] Greene JE, Labbe I, Goulding AD, et al. UNCOVER Spectroscopy Confirms the Surprising Ubiquity of Active Galactic Nuclei in Red Sources at z ¿ 5. Astrophys. J.. 2024 Mar;964(1):39.
[155] Labbe I, Greene JE, Bezanson R, et al. UNCOVER: Candidate Red Active Galactic Nuclei at 3 ¡ z ¡ 7 with JWST and ALMA. Astrophys. J.. 2025 Jan;978(1):92.
[156] de Graaff A, Hviding RE, Naidu RP, et al. Little Red Dots host Black Hole Stars: A unified family of gas-reddened AGN revealed by JWST/NIRSpec spectroscopy. arXiv e-prints. 2025 Nov;:arXiv:2511.21820.
[157] Harikane Y. Early galaxies and supermassive black holes discovered by the James webb space telescope. Astrophys. Space Sci.. 2025 Aug;370(8):85.
[158] Greene JE, Labbe I, Goulding AD, et al. UNCOVER Spectroscopy Confirms the Surprising Ubiquity of Active Galactic Nuclei in Red Sources at z ¿ 5. Astrophys. J.. 2024 Mar;964(1):39.
[159] Juodžbalis I, Marconcini C, D'Eugenio F, et al. A direct black hole mass measurement in a Little Red Dot at the Epoch of Reionization. arXiv e-prints. 2025 Aug; :arXiv:2508.21748.
[160] Furtak LJ, Secunda AR, Greene JE, et al. Investigating photometric and spectroscopic variability in the multiply imaged little red dot A2744-QSO1. Astron. Astrophys.. 2025 Jun;698:A227.
[161] Ji X, Maiolino R, Übler H, et al. BlackTHUNDER – A non-stellar Balmer break in a black hole-dominated little red dot at z = 7.04. Mon. Not. R. Astron. Soc.. 2025 Dec; 544(4):3900–3935.
[162] Newman AB, Gu M, Belli S, et al. A stellar dynamical mass measure of an inactive black hole in the distant universe. arXiv e-prints. 2025 Mar;:arXiv:2503.17478.
[163] Zhang Z, Li M, Oguri M, et al. Little red dot variability over a century reveals black hole envelope via a giant Einstein cross. arXiv e-prints. 2025 Dec;:arXiv:2512.05180.
[164] Baggen JFW, Scoggins MT, van Dokkum P, et al. Connecting the Dots: UV-Bright Companions of Little Red Dots as Lyman-Werner Sources Enabling Direct Collapse Black Hole Formation. arXiv e-prints. 2026 Feb;:arXiv:2602.02702.
[165] Golubchik M, Furtak LJ, Allingham JFV, et al. VENUS: When Red meets Blue – A multiply imaged Little Red Dot with an apparent blue companion behind the galaxy

cluster Abell 383. arXiv e-prints. 2025 Dec;:arXiv:2512.02117.
[166] Yanagisawa H, Ouchi M, Golubchik M, et al. VENUS: Two Faint Little Red Dots Separated by ~ 70 pc Hidden in a Single Lensed Galaxy at $z \sim 7$. arXiv e-prints. 2026 Jan; :arXiv:2601.06015.
[167] Yanagisawa H, Ouchi M, Golubchik M, et al. VENUS: Two Faint Little Red Dots Separated by ~ 70 pc Hidden in a Single Lensed Galaxy at $z \sim 7$. arXiv e-prints. 2026 Jan; :arXiv:2601.06015.
[168] Zhang Z, Li M, Oguri M, et al. Little red dot variability over a century reveals black hole envelope via a giant Einstein cross. arXiv e-prints. 2025 Dec;:arXiv:2512.05180.
[169] Sharon K, Gladders MD, Rigby JR, et al. Source-plane Reconstruction of the Bright Lensed Galaxy RCSGA 032727-132609. Astrophys. J.. 2012 Feb;746(2):161.
[170] Zitrin A, Broadhurst T, Coe D, et al. Strong-lensing analysis of MS 1358.4+6245: New multiple images and implications for the well-resolved z= 4.92 galaxy. Mon. Not. R. Astron. Soc.. 2011 May;413:1753–1763.
[171] Law DR, Shapley AE, Steidel CC, et al. High velocity dispersion in a rare grand-design spiral galaxy at redshift z = 2.18. Nature. 2012 Jul;487(7407):338–340.
[172] Costantin L, Pérez-González PG, Guo Y, et al. A Milky Way-like barred spiral galaxy at a redshift of 3. Nature. 2023 Nov;623(7987):499–501.
[173] Kuhn V, Guo Y, Martin A, et al. JWST Reveals a Surprisingly High Fraction of Galaxies Being Spiral-like at $0.5 \leq z \leq 4$. Astrophys. J. Lett.. 2024 Jun;968(2):L15.
[174] Xiao M, Williams CC, Oesch PA, et al. PANORAMIC: Discovery of an ultra-massive grand-design spiral galaxy at $z \sim 5.2$. Astron. Astrophys.. 2025 Apr;696:A156.
[175] Wang W, Cantalupo S, Pensabene A, et al. A giant disk galaxy two billion years after the Big Bang. Nature Astronomy. 2025 May;9:710–719.
[176] Jain R, Wadadekar Y. A grand-design spiral galaxy 1.5 billion years after the Big Bang with JWST. Astron. Astrophys.. 2025 Nov;703:A96.
[177] Allingham JFV, Zitrin A, Kokorev V, et al. VENUS: Strong-lensing model of MACS J1931.8-2635 – revealing the farthest multiply imaged supernova. arXiv e-prints. 2026 Feb;:arXiv:2602.14074.
[178] Claeyssens A, Adamo A, Richard J, et al. Star formation at the smallest scales: a JWST study of the clump populations in SMACS0723. Mon. Not. R. Astron. Soc.. 2023 Apr; 520(2):2180–2203.
[179] Portegies Zwart SF, McMillan SLW, Gieles M. Young Massive Star Clusters. Annu. Rev. Astron. Astrophys.. 2010 Sep;48:431–493.
[180] Claeyssens A, Adamo A, Kokorev V, et al. A first GLIMPSE into star clusters populations across cosmic time. arXiv e-prints. 2026 Jan;:arXiv:2601.16281.
[181] Adamo A, Hollyhead K, Messa M, et al. Star cluster formation in the most extreme environments: insights from the HiPEEC survey. Mon. Not. R. Astron. Soc.. 2020 Dec; 499(3):3267–3294.
[182] Mowla L, Iyer KG, Desprez G, et al. The Sparkler: Evolved High-redshift Globular Cluster Candidates Captured by JWST. Astrophys. J. Lett.. 2022 Oct;937(2):L35.
[183] Abdurro'uf, Coe D, Resseguier T, et al. Spatially Resolved Physical Properties of Young Star Clusters and Star-forming Clumps in the Brightest z¿6 Galaxy, the Strongly Lensed Cosmic Spear at z=6.2. arXiv e-prints. 2025 Dec;:arXiv:2512.08054.
[184] Bradač M, Judež J, Willott C, et al. Star Formation under a Cosmic Microscope: Highly Magnified z = 11 Galaxy behind the Bullet Cluster. Astrophys. J. Lett.. 2025 Dec; 995(2):L74.
[185] Adamo A, Bradley LD, Vanzella E, et al. Bound star clusters observed in a lensed galaxy 460 Myr after the Big Bang. Nature. 2024 Aug;632(8025):513–516.
[186] Hsiao TYY, Coe D, Abdurro'uf, et al. JWST Reveals a Possible $z \sim 11$ Galaxy Merger in Triply Lensed MACS0647-JD. Astrophys. J. Lett.. 2023 Jun;949(2):L34.
[187] Vanzella E, Claeyssens A, Welch B, et al. JWST/NIRCam Probes Young Star Clusters in the Reionization Era Sunrise Arc. Astrophys. J.. 2023 Mar;945(1):53.
[188] Fujimoto S, Ouchi M, Kohno K, et al. Primordial rotating disk composed of at least 15

dense star-forming clumps at cosmic dawn. Nature Astronomy. 2025 Aug;9:1553–1567.
[189] Miralda-Escude J. The Magnification of Stars Crossing a Caustic. I. Lenses with Smooth Potentials. Astrophys. J.. 1991 Sep;379:94.
[190] Kelly PL, Diego JM, Rodney S, et al. Extreme magnification of an individual star at redshift 1.5 by a galaxy-cluster lens. Nature Astronomy. 2018 Apr;2:334–342.
[191] Windhorst RA, Timmes FX, Wyithe JSB, et al. On the Observability of Individual Population III Stars and Their Stellar-mass Black Hole Accretion Disks through Cluster Caustic Transits. Astrophys. J. Suppl. Ser.. 2018 Feb;234:41.
[192] Venumadhav T, Dai L, Miralda-Escudé J. Microlensing of Extremely Magnified Stars near Caustics of Galaxy Clusters. Astrophys. J.. 2017 Nov;850:49.
[193] Diego JM, Kaiser N, Broadhurst T, et al. Dark Matter under the Microscope: Constraining Compact Dark Matter with Caustic Crossing Events. Astrophys. J.. 2018 Apr; 857:25.
[194] Oguri M, Diego JM, Kaiser N, et al. Understanding caustic crossings in giant arcs: Characteristic scales, event rates, and constraints on compact dark matter. Phys. Rev. D. 2018 Jan;97(2):023518.
[195] Meena AK, Li SK, Zitrin A, et al. Flashlights: Prospects for constraining the initial mass function around cosmic noon with caustic-crossing events. Astron. Astrophys.. 2025 Jul; 699:A299.
[196] Li SK, Diego JM, Meena AK, et al. Constraining the z $\sim$ 1 Initial Mass Function with HST and JWST Lensed Stars in MACS J0416.1−2403. Astrophys. J.. 2025 Aug; 988(2):178.
[197] Chen W, Kelly PL, Diego JM, et al. Searching for Highly Magnified Stars at Cosmological Distances: Discovery of a Redshift 0.94 Blue Supergiant in Archival Images of the Galaxy Cluster MACS J0416.1-2403. Astrophys. J.. 2019 Aug;881(1):8.
[198] Kaurov AA, Dai L, Venumadhav T, et al. Highly Magnified Stars in Lensing Clusters: New Evidence in a Galaxy Lensed by MACS J0416.1-2403. Astrophys. J.. 2019 Jul; 880(1):58.
[199] Meena AK, Zitrin A, Jiménez-Teja Y, et al. Two Lensed Star Candidates at $z \simeq 4.8$ behind the Galaxy Cluster MACS J0647.7+7015. Astrophys. J. Lett.. 2023 Feb;944(1):L6.
[200] Golubchik M, Zitrin A, Pierel J, et al. A search for transients in the Reionization Lensing Cluster Survey (RELICS): three new supernovae. Mon. Not. R. Astron. Soc.. 2023 Jul; 522(3):4718–4727.
[201] Meena AK, Arad O, Zitrin A. An efficient method for simulating light curves of cosmological microlensing and caustic crossing events. Mon. Not. R. Astron. Soc.. 2022 Aug; 514(2):2545–2560.
[202] Meena AK, Chen W, Zitrin A, et al. Flashlights: an off-caustic lensed star at redshift z = 1.26 in Abell 370. Mon. Not. R. Astron. Soc.. 2023 Jun;521(4):5224–5231.
[203] Welch B, Coe D, Diego JM, et al. A highly magnified star at redshift 6.2. Nature. 2022 Mar;603(7903):815–818.
[204] Welch B, Coe D, Zackrisson E, et al. JWST Imaging of Earendel, the Extremely Magnified Star at Redshift z = 6.2. Astrophys. J. Lett.. 2022 Nov;940(1):L1.
[205] Pascale M, Dai L, Frye BL, et al. Is Earendel a Star Cluster?: Metal-poor Globular Cluster Progenitors at z $\sim$ 6. Astrophys. J. Lett.. 2025 Aug;988(2):L76.
[206] Furtak LJ, Meena AK, Zackrisson E, et al. Reaching for the stars - JWST/NIRSpec spectroscopy of a lensed star candidate at z = 4.76. Mon. Not. R. Astron. Soc.. 2024 Jan;527(1):L7–L13.
[207] Meena AK, Bagla JS. Exotic image formation in strong gravitational lensing by clusters of galaxies - IV. Elliptical NFW lenses and hyperbolic umbilics. Mon. Not. R. Astron. Soc.. 2023 Dec;526(3):3902–3919.
[208] Rivera-Thorsen TE, Chisholm J, Welch B, et al. The Sunburst Arc with JWST: I. Detection of Wolf-Rayet stars injecting nitrogen into a low-metallicity, z = 2.37 proto-globular cluster leaking ionizing photons. Astron. Astrophys.. 2024 Oct;690:A269.
[209] Pascale M, Dai L. A Young Super Star Cluster Powering a Nebula of Retained Massive

Star Ejecta. Astrophys. J.. 2024 Dec;976(2):166.
[210] Fudamoto Y, Sun F, Diego JM, et al. Identification of more than 40 gravitationally magnified stars in a galaxy at redshift 0.725. Nature Astronomy. 2025 Mar;9:428–437.
[211] Refsdal S. On the possibility of determining Hubble's parameter and the masses of galaxies from the gravitational lens effect. Mon. Not. R. Astron. Soc.. 1964;128:307.
[212] Kelly PL, Rodney SA, Treu T, et al. Multiple images of a highly magnified supernova formed by an early-type cluster galaxy lens. Science. 2015 Mar;347:1123–1126.
[213] Rodney SA, Strolger LG, Kelly PL, et al. SN Refsdal: Photometry and Time Delay Measurements of the First Einstein Cross Supernova. Astrophys. J.. 2016 Mar;820:50.
[214] Kelly PL, Rodney S, Treu T, et al. Constraints on the Hubble constant from supernova Refsdal's reappearance. Science. 2023 Jun;380(6649):abh1322.
[215] Ofek EO, Rabinak I, Neill JD, et al. Supernova PTF 09UJ: A Possible Shock Breakout from a Dense Circumstellar Wind. Astrophys. J.. 2010 Dec;724(2):1396–1401.
[216] Waxman E, Katz B. Shock Breakout Theory. In: Alsabti AW, Murdin P, editors. Handbook of supernovae; 2017. p. 967.
[217] Rodney SA, Brammer GB, Pierel JDR, et al. A gravitationally lensed supernova with an observable two-decade time delay. Nature Astronomy. 2021 Nov;5:1118–1125.
[218] Chen W, Kelly PL, Oguri M, et al. Shock cooling of a red-supergiant supernova at redshift 3 in lensed images. Nature. 2022 Nov;611(7935):256–259.
[219] Rodney SA, Balestra I, Bradac M, et al. Two peculiar fast transients in a strongly lensed host galaxy. Nature Astronomy. 2018 Apr;2:324–333.
[220] Dhanasingham B, Kelly PL, Chen W, et al. SN 2022riv in RX J2129: Discovery, Spectroscopic Classification, and Microlensing of a Strongly Lensed Type Ia Supernova from JWST and HST Observations. arXiv e-prints. 2026 Apr;:arXiv:2604.11882.
[221] Pierel JDR, Newman AB, Dhawan S, et al. Lensed Type Ia Supernova "Encore" at z = 2: The First Instance of Two Multiply Imaged Supernovae in the Same Host Galaxy. Astrophys. J. Lett.. 2024 Jun;967(2):L37.
[222] Frye BL, Pascale M, Pierel J, et al. The JWST Discovery of the Triply Imaged Type Ia "Supernova H0pe" and Observations of the Galaxy Cluster PLCK G165.7+67.0. Astrophys. J.. 2024 Feb;961(2):171.
[223] Larison C, Pierel J, Coulter D, et al. The Strongly Lensed Supernova Pantheon As Revealed by JWST. In: American Astronomical Society Meeting Abstracts; (American Astronomical Society Meeting Abstracts; Vol. 247); Feb.; 2026. p. 156.06.
[224] Coulter DA, Larison C, Pierel JDR, et al. A spectroscopically confirmed, strongly lensed, metal-poor Type II supernova at z = 5.13. arXiv e-prints. 2026 Jan;:arXiv:2601.04156.
[225] Mahler G, Jauzac M, Edge AC, et al. JWST Cluster SLICE - Strong LensIng and Cluster Evolution [Jwst proposal. cycle 3, id. #5594]; 2024.
[226] Cerny C, Mahler G, Sharon K, et al. Strong LensIng and Cluster Evolution (SLICE) with JWST: Early Results, Lens Models, and High-redshift Detections. Astrophys. J.. 2026 Apr;1001(1):60.
[227] Diego JM, Goolsby C, Conselice CJ, et al. A tight relation between the distribution of globular clusters and dark matter in AS1063. arXiv e-prints. 2026 Feb;:arXiv:2602.12332.
[228] Keatley KE, Harris WE. JWST NIRCam Observations of the Globular Cluster Population of RXJ 2129.7+0005. Astrophys. J.. 2025 Sep;990(1):67.
[229] Hinrichs TR, Kamieneski PS, Windhorst RA, et al. Hidden in Plain Sight: Searching for Globular Clusters within JWST Observations of the PLCK G165.7+67.0 Galaxy Cluster. Astrophys. J.. 2026 Apr;1001(1):91.
[230] Finner K, Faisst A, Chary RR, et al. The First Weak-lensing Analysis with the James Webb Space Telescope: SMACS J0723.3-7327. Astrophys. J.. 2023 Aug;953(1):102.
[231] Harvey DR, Massey R. Weak gravitational lensing measurements of Abell 2744 using JWST and shear measurement algorithm pyRRG-JWST. Mon. Not. R. Astron. Soc.. 2024 Apr;529(2):802–809.
[232] Cha S, HyeongHan K, Scofield ZP, et al. Precision MARS Mass Reconstruction of A2744: Synergizing the Largest Strong-lensing and Densest Weak-lensing Data Sets from JWST.

Astrophys. J.. 2024 Feb;961(2):186.
[233] Foo N, Harrington KC, Frye BL, et al. PASSAGES: The Discovery of a Strongly Lensed Protocluster Core Candidate at Cosmic Noon. Astrophys. J.. 2025 Dec;995(2):219.
[234] Bogdán Á, Schellenberger G, Li Q, et al. An X-ray-emitting protocluster at z $\asymp$ 5.7 reveals rapid structure growth. Nature. 2026 Jan;649(8099):1134–1138.
[235] Morishita T, Roberts-Borsani G, Treu T, et al. Early Results from GLASS-JWST. XIV. A Spectroscopically Confirmed Protocluster 650 Million Years after the Big Bang. Astrophys. J. Lett.. 2023 Apr;947(2):L24.
[236] Laporte N, Zitrin A, Dole H, et al. A lensed protocluster candidate at z = 7.66 identified in JWST observations of the galaxy cluster SMACS0723–7327. Astron. Astrophys.. 2022 Nov;667:L3.
[237] Wu CKW, Ling CT, Goto T, et al. Photometrically selected protocluster candidates at in the JWST COSMOS-Web field. Publ. Astron. Soc. Aust.. 2025 Nov;42:e141.
[238] Fudamoto Y, Helton JM, Lin X, et al. SAPPHIRES: A Galaxy Over-Density in the Heart of Cosmic Reionization at $z = 8.47$. arXiv e-prints. 2025 Mar;:arXiv:2503.15597.
[239] Brammer G, Strait V, Matharu J, et al. grizli ; 2022. Please cite this software using these metadata.; Available from: `https://doi.org/10.5281/zenodo.6672538`.